VYSOKÉ UČENÍ TECHNICKÉ V BRNĚ

BRNO UNIVERSITY OF TECHNOLOGY

FAKULTA STROJNÍHO INŽENÝRSTVÍ
ENERGETICKÝ ÚSTAV

FACULTY OF MECHANICAL ENGINEERING
ENERGY INSTITUTE

KVALITA ROZPRAŠOVÁNÍ PALIV U MALÝCH TLAKOVÝCH VÍŘIVÝCH TRYSEK

QUALITY OF FUEL ATOMIZATION FROM SMALL PRESSURE-SWIRL ATOMIZERS

BAKALÁŘSKÁ PRÁCE
BACHELOR'S THESIS

AUTOR PRÁCE — MILAN MALÝ
AUTHOR

VEDOUCÍ PRÁCE — doc. Ing. JAN JEDELSKÝ, Ph.D.
SUPERVISOR

BRNO 2014

Vysoké učení technické v Brně, Fakulta strojního inženýrství

Energetický ústav
Akademický rok: 2013/2014

ZADÁNÍ BAKALÁŘSKÉ PRÁCE

student(ka): Milan Malý

který/která studuje v **bakalářském studijním programu**

obor: **Strojní inženýrství (2301R016)**

Ředitel ústavu Vám v souladu se zákonem č.111/1998 o vysokých školách a se Studijním a zkušebním řádem VUT v Brně určuje následující téma bakalářské práce:

Kvalita rozprašování paliv u malých tlakových vířivých trysek

v anglickém jazyce:

Quality of fuel atomization from small pressure-swirl atomizers

Stručná charakteristika problematiky úkolu:

Tlakové vířivé trysky (TVT) jsou používány v mnoha aplikacích, např. pro rozprašování paliv ve spalovacích motorech různých typů. Tato klasická koncepce podléhá i v současnosti inovacím pro zvýšení technické hodnoty motoru jako celku. Struktura a geometrie spreje, velikost a rychlost generovaných kapek patří mezi důležité a sledované parametry trysek, které budou na konkrétní trysce zkoumány pomocí optických měřících metod.

Cíle bakalářské práce:

- rešerše relevantních publikací k TVT
- Úprava zkušebního zařízení pro provoz malých TVT, ověření přesnosti snímačů provozních veličin
- Příprava a nastavení optického měřícího systému
- Měření vybraných vlastností spreje u jedné, případně více TVT
- Analýza výsledků, popis spreje a vyhodnocení vlivu provozních podmínek. Grafická prezentace výsledků.

Seznam odborné literatury:

[1] Bayel, L., Orzechowski, Z., Liquid atomization, Taylor & Francis, Washington, D.C., 1993
[2] Khavkin, Y., The Theory and Practice of Swirl Atomizers, Taylor & Francis, 2004 - Počet stran: 462
[3] Kopecký, V. Laserová anemometrie v mechanice tekutin, 2008, česky, Tribun EU / Knihovnicka.cz, Brno, 205 stran, ISBN: 9788073993573
[4] ZHANG, Zh., LDA Application Methods: Laser Doppler Anemometry for Fluid Dynamics (Experimental Fluid Mechanics), Springer, ISBN: 9783642135132, 2010.
[5] Dantec dynamics - firemní literatura

Summary

The present thesis deals with measurement of spray characteristics of pressure-swirl atomizer by Phase Doppler Anemometry (PDA). The aim of these measurements is to investigate and compare spray characteristics using different liquids and different regimes of inlet pressure and determine if it is possible to replace kerosene with biofuels in terms of quality of atomization.

The theoretical part deals with fundamental basics of the atomization of pressure-swirl atomizers and the principles of laser anemometry. The experimental part describes test bench, operating regiments and the setup of the experiment. Results contain visualization of spray, droplet size distribution inside spray, velocity and Sauter mean diameter (SMD) profile in various operation conditions as different downstream distance, various inlet pressure and different liquids.

Keywords: PDA, Phase Doppler anemometry, droplet, atomization, atomizer, spray, swirl, simplex,

Abstrakt

Tato bakalářská práce se zabývá měřením charakteristik spreje z tlakové vířivé trysky za použití fázového doplerovského analyzátoru. Cílem měření bylo stanovit a porovnat charakteristiky spreje za použití různých kapalin a různých režimů tlaků a rozhodnout, jestli je možné nahradit kerosin biopalivy z pohledu kvality atomizace.

Teoretická část se zabývá základy rozpadu kapalin z tlakových vířivých trysek a principy laserové anemometrie. Experimentální část popisuje testovací trať, provozní podmínky a nastavení experimentu. Výsledy obsahují vizualizaci spreje, velikostní rozložení kapek uvnitř spreje a profily rychlosti a Sautrova středního průměru za použití různých provozních podmínek jako je různá vzdálenost od trysky, rozdílný vstupní tlak a různé kapaliny.

Klíčová slova: PDA, Fázový doplerovský analyzátor, kapka, rozpad, tryska, sprej, vířivý, jednoduchý

Bibliographic citation

MALÝ, M. *Kvalita rozprašování paliv u malých tlakových vířivých trysek.* Brno: Vysoké učení technické v Brně, Fakulta strojního inženýrství, 2014. 52 s. Vedoucí bakalářské práce doc. Ing. Jan Jedelský, Ph.D.

Affirmation

I declare that this bachelor's thesis is the result of my own work led by doc. Ing. Jan Jedelský, Ph.D. and all used sources are duly listed in the bibliography.

Milan Malý

Preface

Liquid atomization plays an important role in many technical applications such as gas turbines, engines, spray drying, cooling etc. Each application requires atomizers with different design and operating conditions. Quality of atomization plays significant role in the most of combustion processes. The Sauter mean diameter (SMD) is one of the main characteristics of the atomizer. The aim is to achieve as small SMD as possible for the reason that atomizer with higher SMD produces more pollutions and efficiency of combustor decreases.

The goals of this thesis are:

- Study of relevant publications to pressure-swirl atomizers
- Modification of test equipment for the operation of pressure-swirl atomizers and verification the accuracy of the sensors
- Preparation and setup of optical measuring system
- Measurement of selected characteristics of pressure-swirl atomizer
- Analysis of results, spray description and evaluation the operating conditions. Graphical presentation of results

This thesis is focused on the measurement of spray characteristics of pressure-swirl atomizers for a small-sized jet engine. The possibility of substituting kerosene by biofuels and its effect on the quality of the spray is investigated. The nonintrusive method Phase Doppler Anemometry was used to measure droplets characteristics such as their velocity and size.
This thesis consists of 7 chapters. In the first chapter, a brief description of basics of atomization is presented. The second chapter interprets pressure-swirl atomizers. Chapter 3 deals with the basics of laser Doppler anemometry. Chapter 4 represents test bench and chapter 5 describes an experimental setup. The results of measurement are examined and discussed in chapter 6. The last chapter concludes this thesis.

Acknowledgments

Foremost, I would like to express my sincere gratitude to my supervisor doc. Ing. Jan Jedelský Ph.D. for his patience, motivation, enthusiasm, and immense knowledge.

I am also grateful that I had the opportunity to work with equipment provided for research and scientific activities of NETME Centre, regional R&D centre built with the financial support from the Operational Programme Research and Development for Innovations within the project NETME Centre (New Technologies for Mechanical Engineering), Reg. No. CZ.1.05/2.1.00/01.0002 and, in the follow-up sustainability stage, supported through NETME CENTRE PLUS (LO1202) by financial means from the Ministry of Education, Youth and Sports under the „National Sustainability Programme I“.

I would like to express my thanks to Ph.D. student Ing. Matouš Zaremba who helped me at the beginning of the operation of the entire measurement system.

Last but not least, I would like to thank my family for the support they have provided me throughout my entire life.

Contents

1. Basics of atomization

This theme was recently two times processed at the Brno University of technology in a Master thesis by Matouš Zaremba and Lukáš Durdina. For this reason the basics of atomization aimed at pressure-swirl atomizers will be described only briefly.

1.1. Introduction

The objective of atomization is to break the liquid (fuel) into small drops. This conversion is important in many industrial processes such as:

- Combustion
- Attemperation of stream
- Water cooling
- Oil mist lubrication
- Liquid metal atomization
- Spray coating
- Washing and cleaning

The whole process of atomization is made of by mechanical energy, which is used to overcome the molecular forces between the liquid particles.

1.2. Classification of atomizers

A device used in the atomization of liquids is called an atomizer or a nozzle. Many various shapes of atomizers are used in practice and their design can be divided into three main groups listed below. None of them is perfect and every atomizer has its advantages and disadvantages over others.

1.2.1. Pressure atomizers

Pressure atomizers are based on the conversion of pressure into kinetic energy to achieve a high relative velocity between fuel and surrounding air. These types of atomizers are the most widely used. Their main benefits are simple construction and no need for additional energy or medium [1, 2].

1.2.2. Twin-fluid atomizers

Most twin fluid atomizers use kinetic energy of pressurized air or stream to shatter liquid into drops. We recognize two different group, air-assist and airblast atomizers. Common advantages of these types are good atomization with low liquid pressure and the ability to atomize more viscous liquid [1].

1.2.3. Other atomizers

In the industry we may encounter a large amount of other atomizers construction like rotary, electrostatic, acoustics, ultrasonic etc. [3]. However, the most commonly used atomizers are described above.

1.2.4. Atomizer requirements

Lefebvre in [2] summarized an atomizer requirements:

1. Good atomization over wide ranges of fuel rates
2. Rapid response to changes in fuel flow rate
3. Freedom from flow instabilities
4. Low pump power requirements
5. Low weight
6. Lowe cost, ease of maintenance, and ease of removal for servicing
7. Low susceptibility to damage during manufacture and installation
8. Low susceptibility to carbon buildup on the nozzle face
9. Close adherence to design spray angle
10. Material selection for resistance to oxidation and erosion
11. Resistance to vibration and fatigue
12. Thermal shielding for life enhancement and protection of fuel
13. Uniformity of fuel spray patternation
14. Time between overhaul of 20 000 h

1.3. Liquid properties

The atomization process is influenced by properties of atomizing liquid (fuel), atomizer geometry and operating conditions. Basic liquid properties are density, viscosity and surface tension.

1.3.1. Liquid density

Liquid density ρ_l is defined as liquid weight per its volume:

$$\rho_l = \frac{m_l}{V_l} \tag{1.1}$$

Where m_l is liquid mass and V_l liquid volume.

The density of commonly used liquid in combustion is between 700 kg/m^3 (gasoline) and 1000 kg/m^3 (heavy heating oil).

1.3.2. Liquid viscosity

We recognize two quantities called viscosity. Dynamic viscosity measures liquid resistance to flow. Viscosity is due to the friction between neighboring particles. It is described by Newton's equation:

$$\tau = \mu \frac{du}{dy} \tag{1.2}$$

Where τ is shear stress, μ is dynamic viscosity and $\frac{du}{dy}$ is derivate of velocity.

The second quantity is known as kinematic viscosity and defined:

$$\vartheta = \frac{\mu}{\rho_l} \tag{1.3}$$

Where μ is dynamic viscosity and ρ is liquid density. Kinematic viscosity is the measure of liquid resistance to flow under the influence of gravity.

The range of viscosity is much larger, than density. Common liquids used in combustion have dynamic viscosity between 0.5 mPa·s (methanol) and up to 1000 mPa·s (residual oils). (Water has dynamic viscosity about 0.9 mPa·s.)

1.3.3. Surface tension

Surface tension is an intermolecular force that acts on the border with liquid volumes to seek to decrease outer surface. It also allows liquid resistance to external forces and its defined:

$$\sigma = \frac{F}{\Delta l} \tag{1.4}$$

Where γ is surface tension, F force along the fluid surface and Δl is the length of the fluid surface. It can also be defined in terms of energy as:

$$\sigma = \frac{dE_A}{dA} \tag{1.5}$$

Where dE_A is the change of surface energy and dA the change of the liquid surface. Surface tension between air and liquid had a range from 22 mN/m (methanol) to 73 mN/m (water). The magnitude of surface tension is smaller than the range of viscosity but higher than the range of density.

1.4. Process of atomization

The atomization process is composed of two separate processes – primary and secondary atomization. In primary atomization the liquid stream is broken up into shreds and ligament via disruptive aerodynamic forces, whereas in secondary atomization these large drops are disintegrated into smaller drops due to restorative surface tension forces. The scheme of atomization of the plain-orifice atomizer is in Figure 1-1. A full description of the whole process of atomization is in Lefebvre [1].

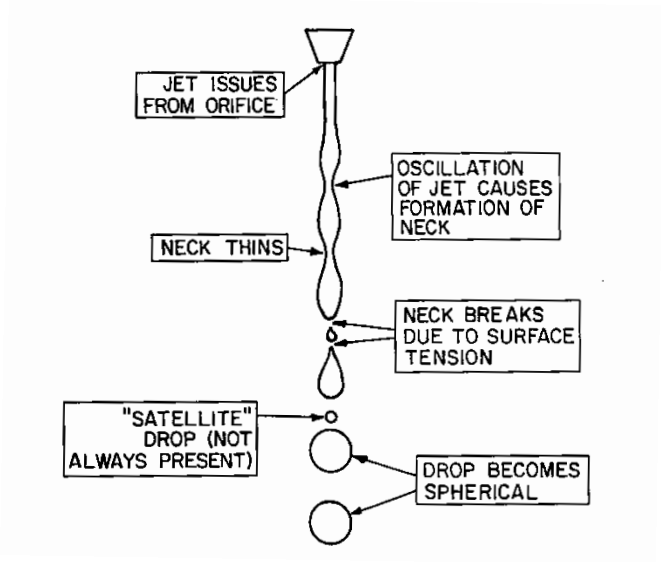

Figure 1-1 Droplet breakup from plain-orifice atomizer [1]

An important parameter in liquid breakup is Weber number, defined as:

$$We = \frac{\rho_l U_0^2 D}{\sigma} \tag{1.6}$$

Where D is droplet diameter and U_0^2 is relative velocity between liquid and air. The Weber number is dimensionless parameter, useful in analysis of fluid flows. The higher the Weber number is, the larger the deforming external pressure forces are, compared with the restoring surface tension [1].

1.4.1. Liquid sheet breakup

For pressure-swirl atomizers is typical generating conical sheet as shown in Figure 1-2. The basics breakup mechanism is similar to the plan-orifice atomizer, the liquid sheet with high relative velocity against the surrounding air is spread into shreds and ligaments that are subsequently disintegrated into droplets. In contrast of the plain-orifice breakup, a wave motion is generated on the liquid sheet, which causes the primary breakup. This process is called classical atomization and is illustrated in Figure 1-3.

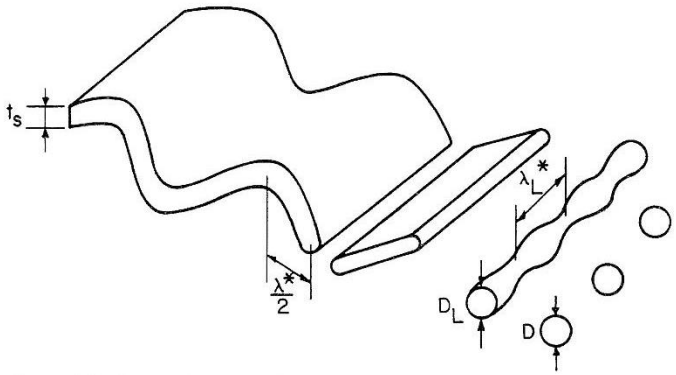

Figure 1-2 Sheet breakup, generated by pressure-swirl atomizer [1]

With increasing inlet pressure and thus relative velocity, sheet breakup occurs closer to the atomizer. At very high relative velocities, atomization starts at the atomizer exit orifice. In this case, the liquid sheet has no time to develop a wavy structure, but is immediately torn into ligaments. This mode is called prompt atomization. For high Weber number prompt atomization is dominant whereas for a low Weber number the classical model is dominant. [1]

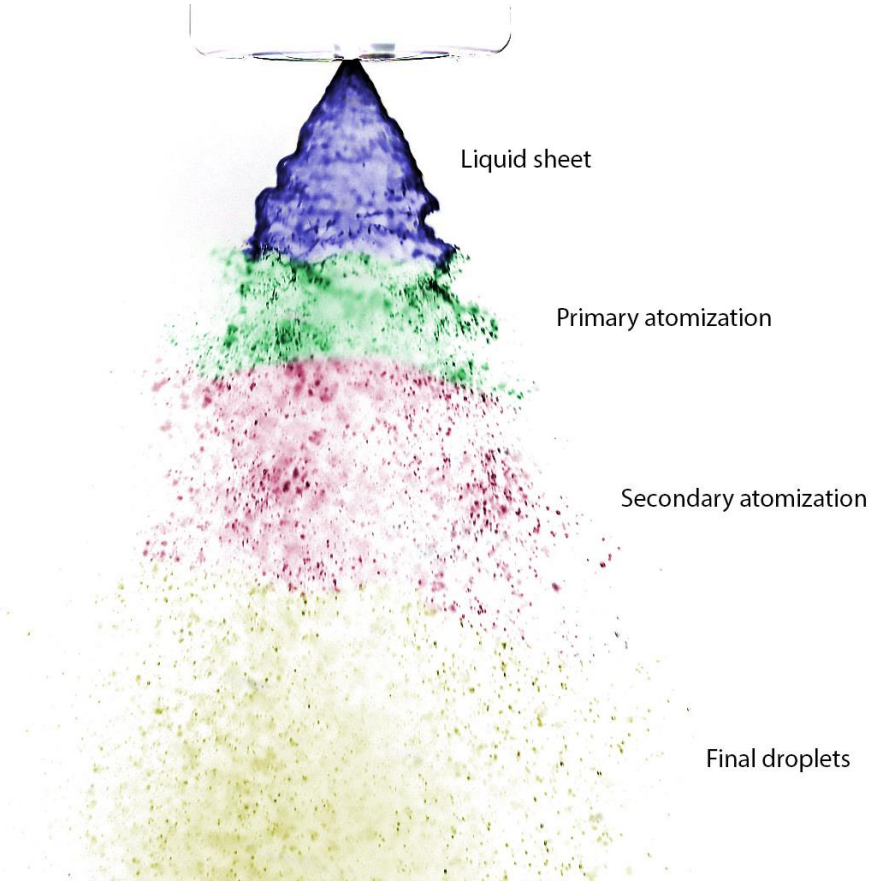

Figure 1-3 Liquid brake up, generated by pressure-swirl atomizer Unijet D1-13 with water at pressure 4 bar. Photo was taken using a Canon D300 with a 100 mm macro lens, expose time 1/80 s, f-stop f2.8, illuminated by background flash. Colored.

1.4.2. Drop size distribution

The atomization process produces droplets with random and chaotic size. Usually, atomizers produce droplets in the size range from a few microns up to several hundred microns. A simple method of illustrating the distribution of drop size in a spray is to plot a histogram, where each bin represents count percent of droplets of a given size class. A histogram sample is shown in Figure 1-4. Because the graphic representation of drop size distribution is experimental, several mathematic models were introduced in an attempt to reduce the intensity of experimental measurements. One of the most commonly used expressions of drop size distribution is described by Rosin and Rammler (1933):

$$1 - Q = \exp\left(-\frac{D}{X}\right)^{q} \tag{1.7}$$

Where Q is the fraction of the total volume contained in drops of diameter less than D and X and q are constants that are determined experimentally. [1]

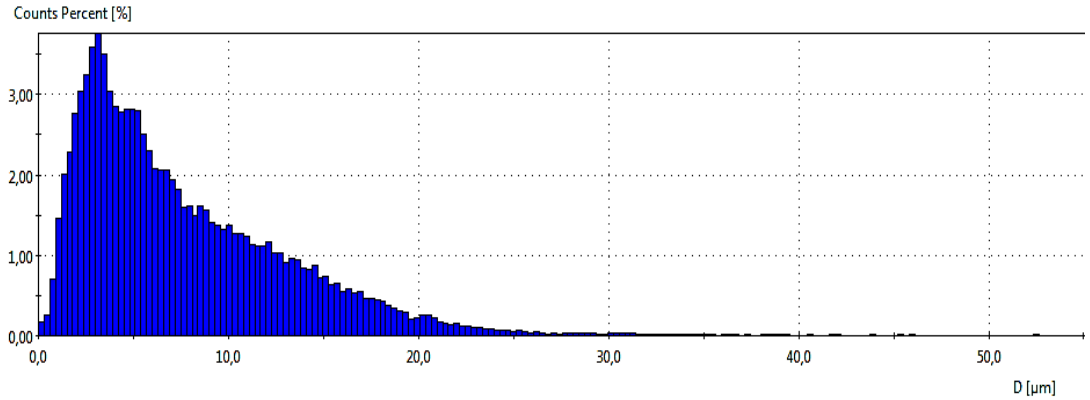

Figure 1-4 Drop size distribution from pressure-swirl atomizer, inlet pressure 10 bar, axial distance from exit orifice 50 mm, in centerline of spray.

For most engineering purposes the distribution of drop sizes may be described in terms of two parameters, one of them is representative diameter (list of representative diameters is in Table 1-1) the other one is a measure of the range of drop sizes.

Table 1-1 Representative diameters, adapted from [1].

$D_{0.1}$	Drop diameter that 10% of total liquid volume is in drops of smaller diameter
$D_{0.5}$	Drop diameter that 50% of total liquid volume is in drops of smaller diameter. Known as mass median diameter (MMD)
$D_{0.632}$	Drop diameter that 63,2% of total liquid volume is in drops of smaller diameter. This is the X parameter in Eq.(1.1)
$D_{0.9}$	Drop diameter that 90% of total liquid volume is in drops of smaller diameter

In many calculations we use only a mean or average diameter instead of the complete drop size distribution. In combustion it is the most important Sauter mean diameter (SMD, named after Josef Sauter in 1924). Generally, a combustor with larger SMD will produce more pollution (oxides of nitrogen, carbon monoxide) [4]. List of list of additional average diameters is in Table 1-2.

Table 1-2 Mean diameters [5].

Common name	Definition	Used for
Arithmetic mean diameter	$D_{10} = \frac{1}{N}\sum_{i=1}^{N_i} n_i D_i$	General comparison and calculating evaporation rates
Area mean diameter	$D_{20} = \left(\frac{1}{N}\sum_{i=1}^{N_i} n_i {D_i}^2\right)^{\frac{1}{2}}$	Monitoring surface applications
Area-length mean diameter	$D_{21} = \frac{\sum_{i=1}^{N_i} n_i {D_i}^2}{\sum_{i=1}^{N_i} n_i D_i}$	Absorption studies
Volume mean diameter	$D_{30} = \left(\frac{1}{N}\sum_{i=1}^{N_i} n_i {D_i}^3\right)^{\frac{1}{3}}$	Hydrology and mass flux applications
Mean evaporative diameter	$D_{31} = \left(\frac{\sum_{i=1}^{N_i} n_i {D_i}^3}{\sum_{i=1}^{N_i} n_i D_i}\right)^{\frac{1}{2}}$	Evaporation and molecular diffusion applications
Sauter mean diameter (SMD)	$D_{32} = \frac{\sum_{i=1}^{N_i} n_i {D_i}^3}{\sum_{i=1}^{N_i} n_i {D_i}^2}$	Mass transfer and reaction
De Broukere diameter	$D_{43} = \frac{\sum_{i=1}^{N_i} n_i {D_i}^4}{\sum_{i=1}^{N_i} n_i {D_i}^3}$	Combustion applications

2. Pressure–swirl atomizer

2.1. Introduction

The design of the pressure-swirl atomizer was introduced by Körting in 1902. This invention has been used for more than a century in many combustion systems. Pressure-swirl atomizers have many advantages over other atomizer types, they are simply constructed, low cost, require small amount energy for atomization and have high reliability. A drawback is the wide dispersion of particle size.

Pressure-swirl atomizers, often called “simplex” due to their simplicity, are basically composed of the swirl chamber with a small exit orifice. Liquid flows into the swirl chamber via tangential ports, rotating in the chamber gains centrifugal forces which lead to the formation of a liquid sheet, which is later disintegrated into ligaments and then into droplets. The two most common spray shapes that result from this process are the hollow-cone design and the full-cone design. The hollow cone design is employed more frequently for its ability to create finer droplets.

2.2. Design of pressure-swirl atomizers

Pressure-swirl atomizers have many design variations. One of the factors is the direction which feeds the liquid. This variation can be divided into the axial and tangential flow design. Tangential design could be called the “true” swirl atomizer, because no special insert is needed. The liquid flows directly into the swirl chamber, meanwhile in axial design the liquid flows through swirl insert, which create the swirl motion in the chamber. Smaller droplets are produced, but there is a disadvantage in clogging of the swirl insert. Both schemes of the designs are shown in fig 2.1. [6].

a) b)

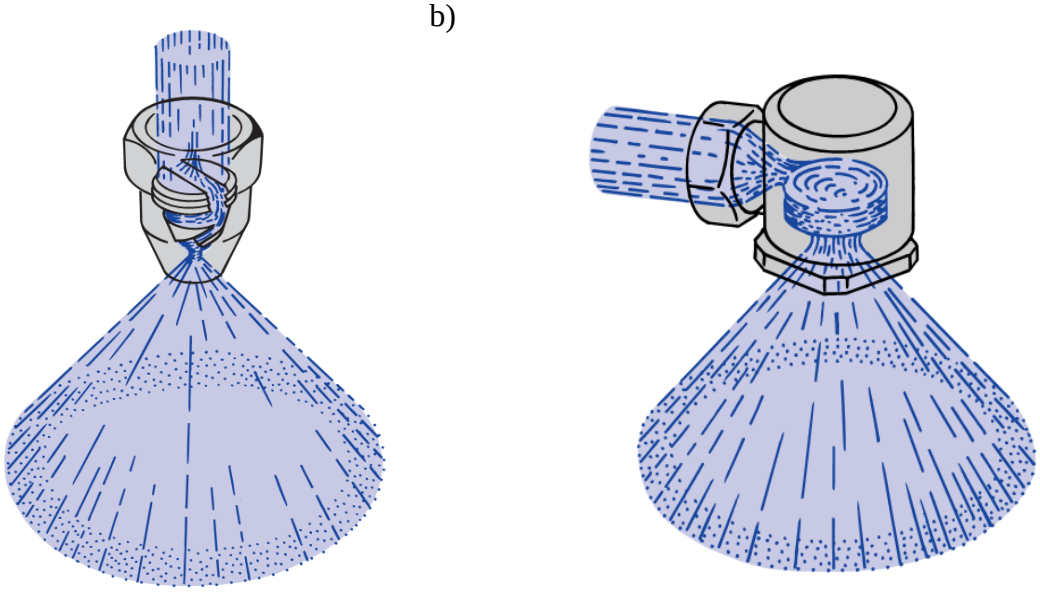

Figure 2-1 a) Schematic of axial flow atomizer, b) schematic of tangential flow atomizer, adapted from [7]

Besides the different design of inputs of fuel, swirl-atomizers can be divided into three main variations: Simplex (described in 2.1), dual-orifice and spill-return.

2.2.1. Spill-return

It is basically a simplex atomizer, except that the rear wall of the swirl chamber contains a passage through which the undue fuel flows back to the fuel tank. The main advantage of the spill return atomizer is that the fuel-injection pressure is always high. It is redeemed by the need for a powerful fuel pump. Another disadvantage of this system is the problematic measuring of the flow rate through the exit orifice. [1]

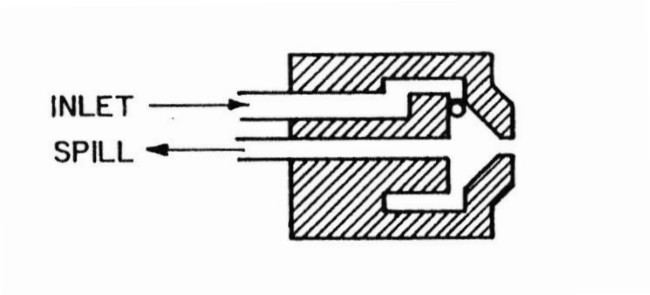

Figure 2-2 Spill return atomizer [1]

2.2.2. Dual-orifice

In brief, a dual-orifice atomizer consists of two simplexes, where one is inside another. At low pressure, the liquid flows through the inner nozzle (primary). As the liquid pressure is increased, distribution valve opens and liquid flows into outer swirl chamber (secondary). The dual-orifice atomizer has a greater working range of liquid pressure than the simplex atomizer. But, when the distribution valve is opening, atomization quality is poor. [1, 3]

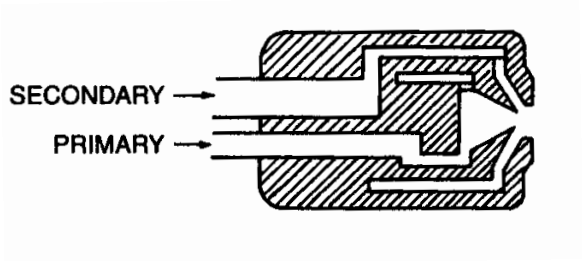

Figure 2-3 Dual-orifice atomizer [1]

2.3. Atomizer characteristics

Atomizer geometry plays a significant role in the quality of atomization, affecting the liquid mass flow rate, liquid sheet thickness, cone angle etc. A list of determining dimensions is shown in Table 2-1 and the schematic layout of the internal geometric is shown in Figure 2-4.

Table 2-1 Atomizer dimensions

Nomenclature	Dimension	Typically unit
D_0	Final orifice diameter	mm
D_c	Swirl chamber diameter	mm
l_c	Length of swirl chamber	mm
l_o	Length of final orifice	mm
A_0	Area of final orifice	mm^2
A_i	Area of inlet holes	mm^2
A_c	Area of swirl chamber	mm^2
2θ	Cone angle	deg

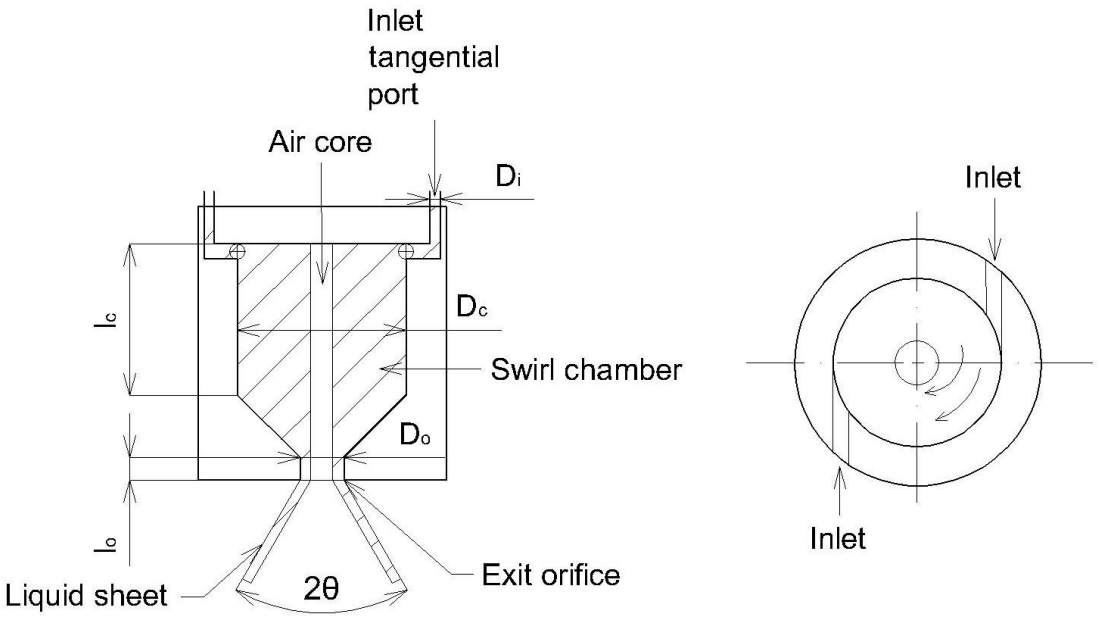

Figure 2-4 Atomizer schematic layout

Several parameters which are depended on the internal geometry are listed below. These parameters are unique to one atomizer.

Flow number

The flow number is a parameter describing the effective flow area of a pressure-swirl atomizer, defined as [1]:

$$FN = \frac{\dot{m}_l}{\sqrt{\rho_l \Delta p_l}} \tag{2.1}$$

Lefebvre in [1] defined the flow number in terms of atomizers dimension as:

$$FN = 0.389 D_o^{1.25} A_i^{0.5} D_c^{-0.25} \tag{2.2}$$

The flow number is an unique parameter for any pressure-swirl atomizer.

Discharge coefficient

The discharge coefficient C_d is the ratio of the actual flow rate to the theoretical flow rate. The C_d of a pressure-swirl atomizer is inevitably low, owing to the presence of the air core, which block off the central portion of the orifice [1]. The discharge coefficient is generally defined as [6]:

$$C_d = \frac{\dot{m}_l}{A_0 \frac{\Delta p_l}{\rho_l}} \tag{2.3}$$

Rizk and Lefebvre in [8] derived a correlation in terms of atomizer dimension as:

$$C_d = 0.35 \left(\frac{A_i}{D_c D_o}\right)^{0.5} \left(\frac{D_c}{D_o}\right)^{0.25} \tag{2.4}$$

Cone angle

An important aspect of atomizer design is the cone angle. In general, increasing of the cone angle lead to an increase in the exposure of the droplets to the surrounding air, which results in improved atomization. Many correlations were made, one of the most complex derived by Rizk and Lefebvre in [9] correlated the atomizer dimensions with liquid properties into equation:

$$2\theta = 6 \left(\frac{D_c D_o}{A_i}\right)^{0.15} \left(\frac{\Delta p_l D_o^2 \rho_l}{\mu_l^2}\right)^{0.25} \tag{2.5}$$

According to equation 2.4, the spray cone angle is widened by increases in the discharge orifice, liquid density and injection pressure. Higher liquid viscosity and larger area of the inlet ports reduce the cone angle.

2.4. SMD prediction

Sauter mean diameter is one of the most discussed atomizer characteristics and plays an important role in combustion process. The goal is to keep SMD as low as possible due to higher efficiency and lower production of pollutions in the combustor.

Many investigations have been undertaken on the performance of swirl nozzles. And still, due to the complex physics in swirl atomization, much has yet to be discovered [3]. A list of the best known empirical correlations of SMD is in Table 2-2, ordered from the oldest to the newest.
The simplest correlations were empirical formulas in the general form [1]:

$$SMD \sim \sigma^a \vartheta^b \dot{m}_l^c \Delta p_l^d \tag{2.6}$$

Where a, b, c, d are experimental constants. Due to a disparity in the listed formulas (I, II, III, VII), it is not possible to define one universal correlation based on this model.

The first equation (I) in Table 2-2 was probably the first correlation of SMD in swirl atomization. It was published by Ohnesorge in 1936 in [10]. He equaled SMD to be a function of injection pressure and mass flow, but does not include any of the liquid properties.

Another correlations were made by Radcliffe [11] (II) and Jasuja [12] (III). They are both very similar to each other. They put in the correlation liquid properties such as viscosity and surface tension. According to the more convenient Lefebvre´s correlation [13] (VII), they have a bigger influence on surface tension and do not involve liquid and air density. These correlations are based on the model from equation 2.6, their advantage is the simplicity of creation and application, but more complex correlations (VIII, IX, X) are more convenient.

Simmons [14] in 1981 investigated six swirl atomizers of small flow rates with water and kerosene and correlated the weber number with inlet pressure. His correlation (IV) is valid only for small atomizers, with a weber of number less than 1.

Babu [15] in 1982 used eight different atomizers for pressure up to 27.6 bar, all with kerosene. He defined three equations (V), which are based on the atomizers dimensions. He also correlated equations for pressure above 27.6 bar, but in this thesis they are not classified.

Kennedy [16] derived his equation (VI) using six different atomizers with 25 types of liquids. He correlated mass flow rate, surface tension and inlet pressure under the condition that the weber number is larger than 10. SMD was found to be independent of liquid viscosity.

Probably one of the most complex, semi-empirical correlation was introduced by Wang and Lefebvre in 1987 in [17]. The equation (VIII) was based on the theory:

$$\mathrm{SMD} = \mathrm{SMD}_1 + \mathrm{SMD}_2 \tag{2.7}$$

Where SMD_1 represents the first stage in the atomization process and SMD_2 represents the final stage of atomization. They used several liquids to provide a range of viscosity from 1 mm^2/s to 18 mm^2/s and range of surface tension from 27 to 73 mN/m. Nowadays, more than quarter-century later, it is taken as a reference for other correlations.

Couto in [18] derived a theoretical formula (IX) based on a hypothesis regarding the thickness of a plane disintegrating liquid sheet. They compared their results with other empirical correlation in their work. They correlated liquid properties with atomizer dimensions and with properties of surrounding air.

Recent investigation was made by Musemic in [19] (X) by testing 20 atomizers a with water-glycerol mixture with a dynamic viscosity of up to 5 mPas. He observed that higher swirl ratio lead to a smaller drop size. A higher swirl ratio means a higher ratio of the tangential velocity component to the axial velocity.

Table 2-2 SMD correlations

N.	Author	Equation	Year	Liquid	Comment
I	Ohnesorge [10]	$SMD = 0.61\dot{m}_l^{0.318}\Delta p_l^{-0.53}$	1936	Water	
II	Radcliffe [11]	$SMD = 7.3\vartheta^{0.2}\sigma^{0.6}\dot{m}_l^{0.25}\Delta p_l^{-0.4}$	1960		ϑ = 0.5-20 mm^2/s ρ_l=750-1600 kg/m^3
III	Jasuja [12]	$SMD = 4.4\vartheta^{0.16}\sigma^{0.6}\dot{m}_l^{0.22}\Delta p_l^{-0.43}$	1979	Kerosene Gas oil Residual fuel oil	
IV	Simmons [14]	$SMD = \Delta p_l{}^{0.275}We^{-0.40}$	1981	Water Kerosene	We <1
V	Babu [15]	$SMD = 170.824\frac{FN^{0.64291}}{\Delta p^{0.22565}}$. $SMD = 198.515\frac{A_0^{0.38888}A_i^{0.32114}}{A_c^{0.05414}\Delta p^{0.2565}}$ $SMD = 66.898\frac{FT^{0.50939}D_0^{1.00546}V_E^{1.01112}}{U_E^{0.0809}\Delta p^{0.72844}}$	1982	Kerosene	Pressure up to 27.6 bar
VI	Kennedy [16]	$SMD = 10^{-3}\sigma(6.11 + 0.32 * 10^5 FN\sqrt{\rho_l} - 6.973x10^{-3}\sqrt{\Delta p_l} + 1.89 * 10^{-6}\Delta p_l)$	1986	25 types of liquids – kerosene, oil, etc.	We > 10
VII	Lefebvre [13]	$SMD = 2.25\mu^{0.25}\sigma^{0.25}\dot{m}_l^{0.22}\Delta p_l^{-0.5}\rho_A^{-0.25}$	1987	Kerosene Gas oil Residual fuel oil	
VIII	Wang, Lefebvre [17]	$SMD = 4.52\left[\frac{\sigma\mu^2}{\rho_A\Delta p_l^2}\right]^{0.25}[t\cos\theta]^{0.25} + 0.39\left[\frac{\sigma\rho_l}{\rho_A\Delta p_l}\right]^{0.25}[t\cos\theta]^{0.75}$	1987	Diesel oil Water	
IX	Couto [18]	$SMD = 1.817\cos\theta\left(\frac{h_0^4\sigma^2}{U_0^4\rho_a\rho_l}\right)^{\frac{1}{6}}\left[1 + 2.6\mu_l\cos\theta\left(\frac{h_0^2\rho_a^4U_0^7}{72\rho_l^2\sigma^5}\right)^{1/3}\right]^{0.2}$	1997	Water Diesel oil	
X	Musemic [19]	$SMD = \left[\frac{k}{We}\right]^{0.44}\left[\frac{\rho_l}{\rho_a}\right]^{0.08}$	2011	Water Water-glycerol	

$t = 3.66\left(\frac{d_0\dot{m}_l\mu_l}{\rho_l\Delta p_l}\right)^{0.25}$ $h_0 = \frac{0.00805FN\sqrt{\rho_l}}{D_0\cos\theta}$ $U_0 = \sqrt{\frac{2\Delta p_l Cd}{\rho_l}}$ $k = \frac{\mu}{2\pi\varphi\sin\left(\frac{\theta}{2}\right)}$

$\varphi = \frac{v_{eff}}{v_{pot}}$

2.5. Conclusion

For combustion is crucial to have as small SMD as possible. From list of correlation in Table 2-2 we can conclude:

- SMD decreases rapidly with increasing liquid pressure
- Increasing liquid viscosity and surface tension lead to increase in SMD significantly
- High density liquid and surrounding air have positive effect on SMD, but this effect is not significant due to small disparity of these values in practice
- Smaller atomizers – with lower flow rate produce smaller SMD
- Wider cone angle reduces SMD

3. Laser anemometry

This chapter shortly describes the basics of laser anemometry used to practical measurements later in this thesis. This topic was described in detail in literature [20-22] and was recently elaborated in a Master thesis by Matouš Zaremba.

3.1. Principle of Laser anemometry

Due to the inability to properly predict or simulate the whole atomization process, a major role is the measurement taken on real atomizers. This measurement provides data used to compare atomizers each other or for computational simulations. There are many different methods to measure the droplet diameter or velocities but probably the most widely used method is Laser Doppler Anemometry (LDA) and its extension Phase Doppler anemometry (PDA). These techniques involve numerous complex physical processes and in this thesis they will be discussed briefly. Several books relating to this topic have been published [20-22].

Laser doppler anemometry is non-intrusive measurement inside fluid flow. It was introduced by Yeh and Cummins [23] in 1964. As the name suggest, it is a technique using laser and the doppler effect for the measurement of particle velocity. Essential to LDA is using of two laser beams, which are collimated, monochromatic, coherent and crossed inside fluid flow. If the beams intersect in their respective beamwaists, consequently the interference produce parallel lighter and darker planes (Figure 3-1) known as fringes [5]. Beams are usually emitted from laser, respectively one beam is emitted and in a beam splitter is divided into two beams.

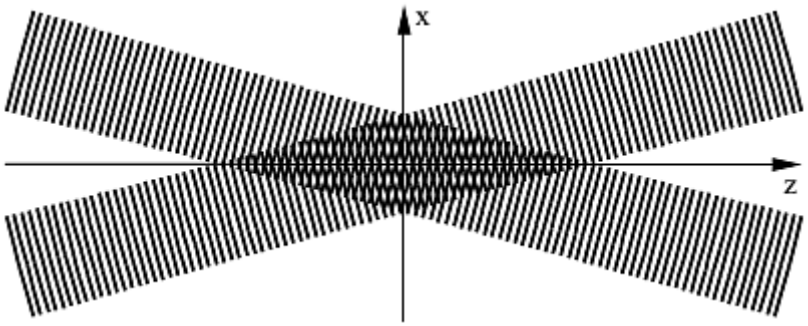

Figure 3-1 Laser beam crossing with fringe pattern [5]

As particles entrained in the fluid pass through the fringes, they reflect light that is then collected by a receiving optics and focused on a photo detector. The current pulse (Figure 3-2) leaving the photo-detector contains the frequency information, which is in computing unit converted to the velocity of the measured particle. As it suggest LDA and indeed PDA can measure only one particle at a time.

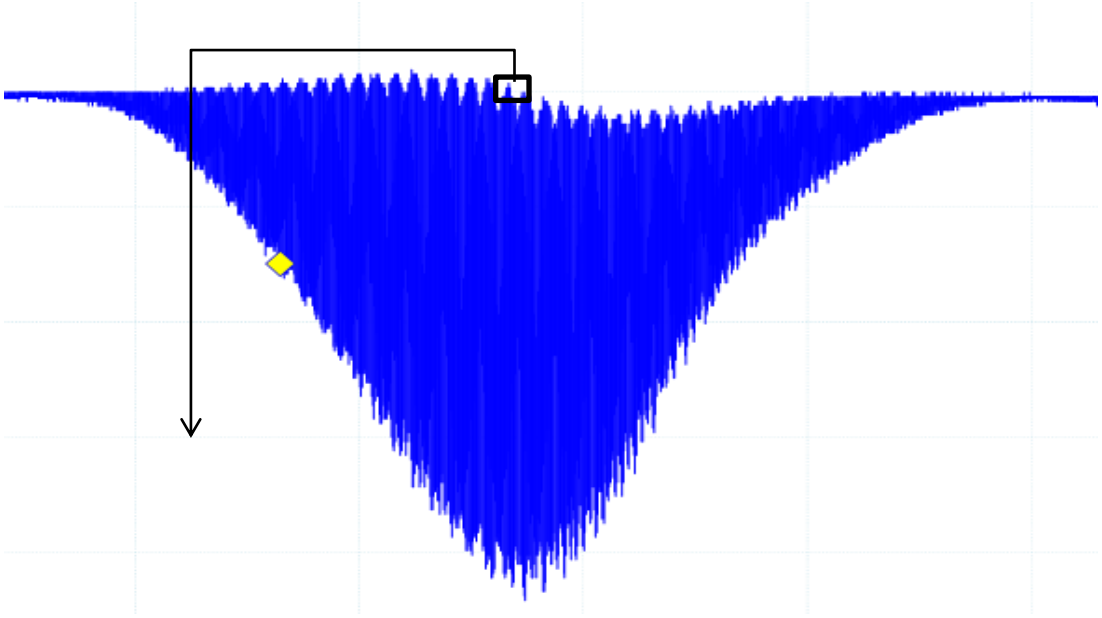

A) Complete current burst from photo detector

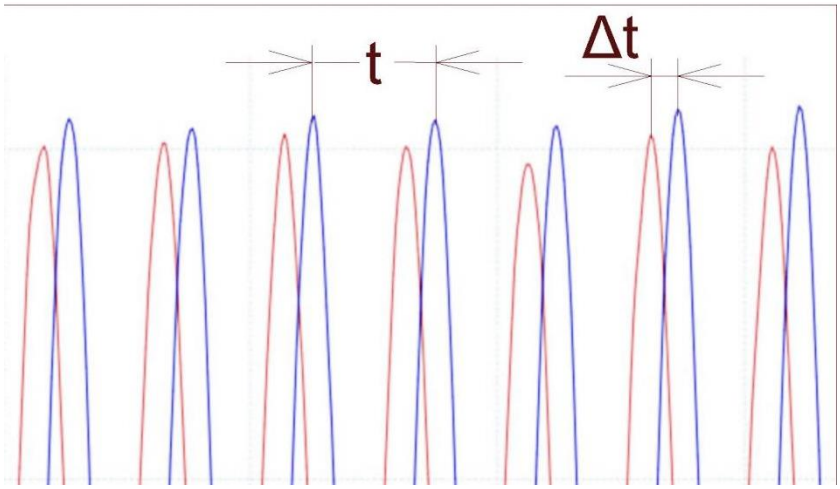

B) Detail of burst from two photo detectors system

Figure 3-2 Current pulse from photo-detector. Shot was made using oscilloscope PicoScope 3405B.

If two velocity components are required, two additional beams must be added to the transmitting optics and an additional detector must be added to the receiving side, which by means of a color separator can detect light solely from the second measurement volume [21]. In order to determine the direction of the particle, one of two beams is shifted by a shift frequency, which is usually 40 MHz. In the fringe model this corresponds to a movement of the fringes. A particle moving with the fringes yields a lower frequency and movement against the fringes, a higher frequency. Frequency shift is made using Bragg cell. The transmitting optic with Bragg cell is shown in Figure 3-3 and it is the same one, used in the PDA measurement later in this thesis.

An Ar-ion laser is commonly used and the emitted beam is not only shifted but also divided by color, where 488 nm (green) is used to measure the axial velocity and, in cases of PDA, also the particle diameter whereas 514 nm (blue) measure radial velocity.

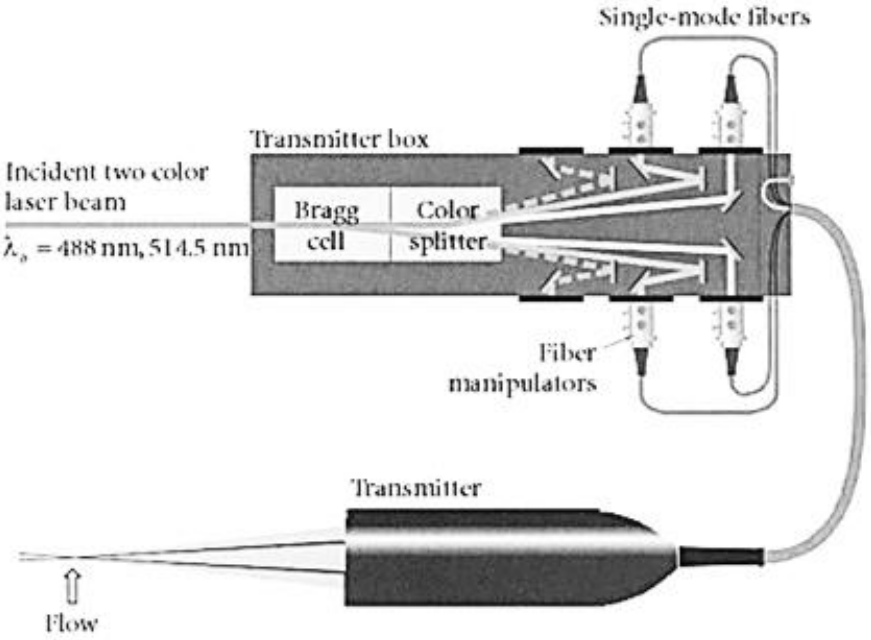

Figure 3-3 Transmitting optic, adapted from [21]

3.2. Phase Doppler anemometry

LDA have only one photo-detector, whereas PDA contains of two or three photo-detectors. Due to different optical path from measuring volume to photo detectors, the phase of the signal is shifted about time shift Δt as shown in Figure 3-2. The magnitude of the Δt is a function of particle size. This function is monotonic and calculable in the case of spherical particles [21]. This technique was introduced by Albrecht et al. in 1993.

The measured data contains information about droplet size, velocity and time when passed through the measuring volume. From these data, mean diameters, data rate and mean velocities are calculated.

4. Test bench

4.1. General description

Some adjustments were made on the old test bench, which was usually operated with twin fluid atomizers. Air supply line was disconnected and a gear pump was mounted into fuel line instead of a pressure vessel. The schematic layout of the new test bench is shown in Figure 4-1.

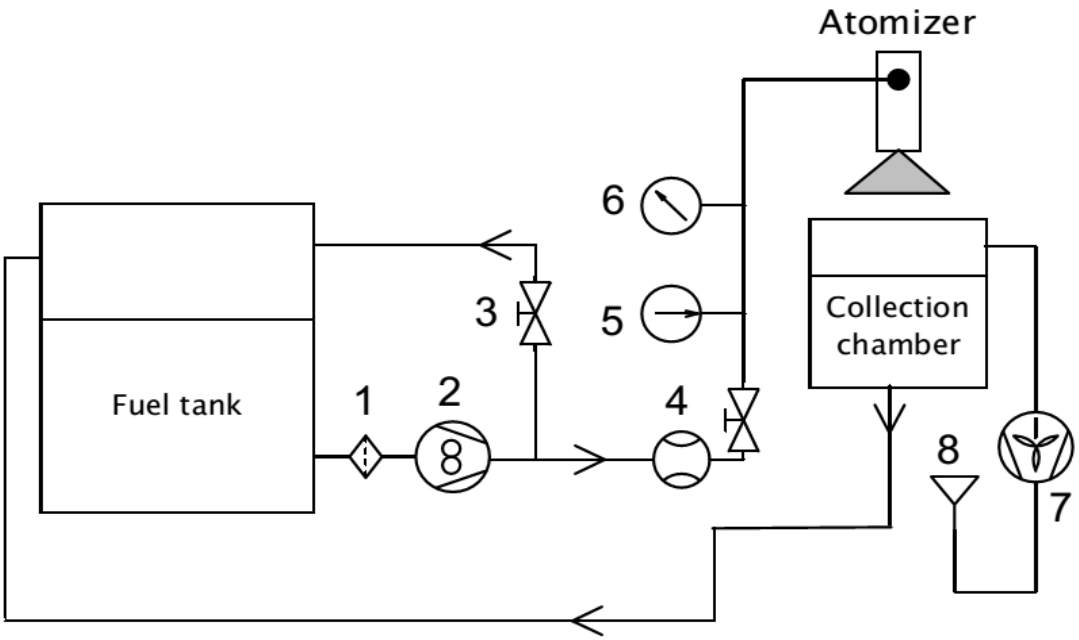

Figure 4-1 Test bench

Liquid fuel is stored in the fuel tank. From the tank is the liquid pumped by a gear pump (2) via filter (1). The mass flow is regulated by regulating the pump speed and fine regulation is made by needle valve (3). The amount of fuel is measured by the mass flow meter (4). Temperature (5) and pressure (6) sensors are also present in the fuel supply system. Atomized liquid is collected by the collection chamber and flows back into the fuel tank. Vapors are ventilated by an axial fan (7) to the central ventilation (8).

4.2. Instrumentation

As shown in Figure 4-1, several measuring instruments were incorporated at test bench to collect important operating parameters like mass flow rate or inlet liquid pressure. Verification of accuracy has been an essential part of the preparation to final measurements.

Flow rate

The flow rate in the main line was measured by Siemens Mass 2100 Di3 Coriolis mass flow meter fitted with a Mass 6000 transmitter. At flow rates above 12.5 kg/h the accuracy declared by manufacturer was ±0.1 % of the actual flow rate. For flow rates below 12.5 kg/h the error could be calculated using the formula:

$$E = \pm\sqrt{0.01 + \frac{1}{\dot{m}_l}} \tag{4.1}$$

Where E is the error of the flow meter in [%] and $\dot{m}_l$ is the actual flow rate [kg/h]. Liquid density is also measured with this device with an error of $\pm 1.5\ kg/m^3$ from the measured value. Flow rate accuracy was verified using the volumetric cylinder and the resulting value was similar to the mass flow meter.

Temperature

The RTD (resistance temperature detector) Omega PR-13 was mounted in the fuel line. An operating range of -30 to 350 °C and an accuracy of $\pm$ 0.2 °C of the actual temperature was declared by the manufacturer. Accuracy was verified using a mercury thermometer and the final deviation was less than 0.2 °C.

Pressure

Pressure was measured with a BD Sensor DMP 331i with a range of 0-18 bar and error was declared by the manufacturer to be less than $\pm$0.35 % of the actual pressure. Error was checked using another pressure sensor and their difference was less than 0.1 %.

5. Setup of experiment

Setup of experiment plays significant role in quality of the results. Essential was to properly align PDA system.

5.1. Phase Doppler Measuring system

For measurement the 2D Fiber PDA system made by Dantec Dynamics was used. The system consists of:

- Spectra physics Stabilite 2017 Argon laser
- 60X41 Transmitter
- 60X81 2D 85 mm Transmitting optics with 50X82 Beam Translator
- 57X50 112 mm diameter fiber PDA receiver optics with spatial filter
- Fiber PDA Detector unit
- BSA P80 Flow and Particle Processor

Schematic layout of used components is drawn in Figure 5-1.

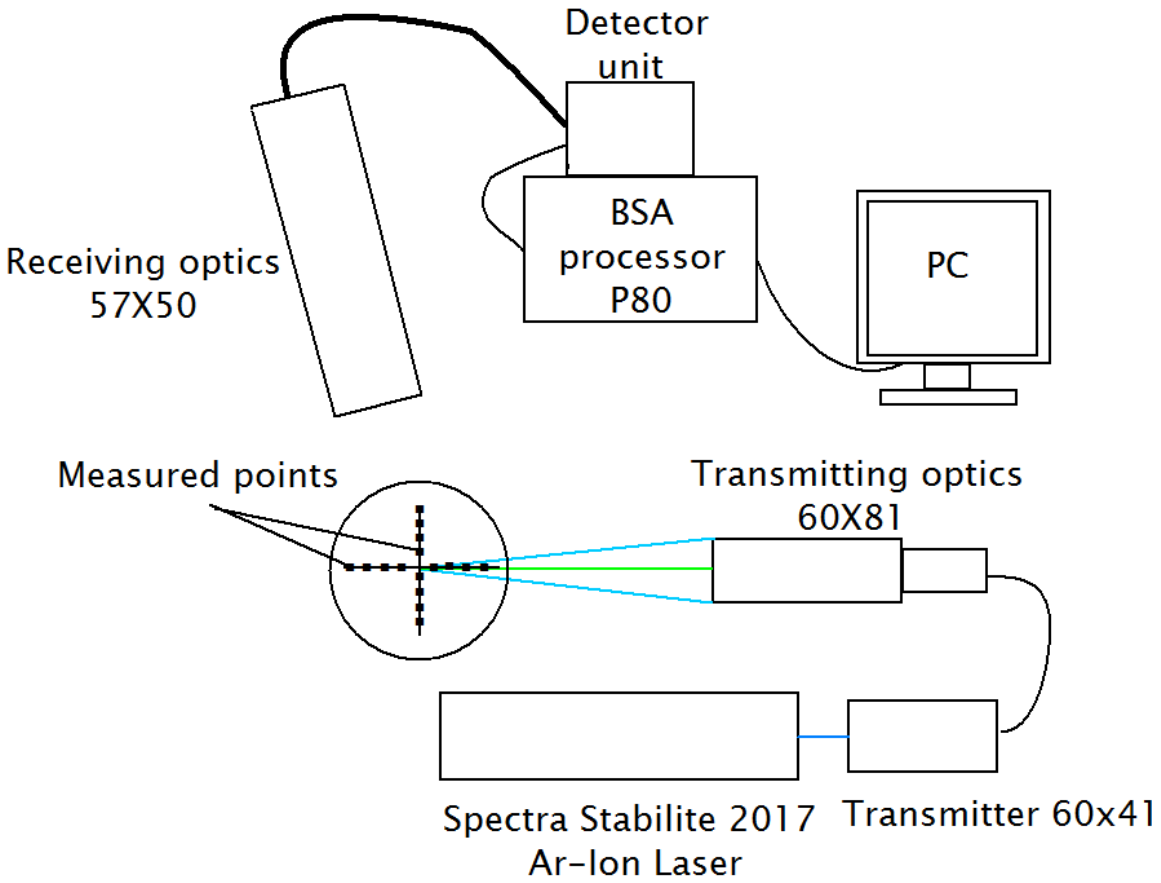

Figure 5-1 PDA schematic layout

Hardware and software setup was made during past year in detail. The main parameters with the greatest influence on measuring quality (validation, data rate etc.) are described below in terms of both hardware and software setup. The others parameters were tested in long-term setup and their influence on measuring are minor.

5.1.1. Hardware setup

Focal lengths were chosen 310 mm for transmitting optics and 500 mm for receiving optics due to the optimal distance from the spray cone. The scattering angle (the angle between the transmitting and receiving optics) was set to 69°. The maximum particle diameter measured by this setup was 105 µm. The spatial filter was set to 0.05 mm. The laser and transmitter box were tuned to their maximum efficiency. The laser aperture was set to value 3 in order to the high quality of the laser beam profile. Laser power was set to 22 A and laser output power is summarized in Table 5-1. Crucial was to set up the blue beams as similarly to each other as possible due to the higher data rate, which was determined by the blue beams.

Table 5-1 Laser power

Laser	**Transmitting optics**			
Output power [mW]	Blue [mW]	Blue shifted [mW]	Green [mW]	Green shifted [mW]
975	53	53	120	96

5.1.2. Software setup

For all measurements BSA flow software v5.1 was used. After hardware adjustment it was necessary to determine the best setting for the software. The main parameters which have influence on the results and their setup are as follows:

- Sensitivity of the photo-detectors: Increases of sensitivity causes a higher data rate but lowers the validation rate. A sensitivity of 800 V for the green channel and 1000 V for the blue channel due to weaker blue laser beam were found to be ideal.
- Signal gain: Gain amplifies the signal from photo-detectors. As sensitivity, a higher data rate is accomplished by increasing the signal gain, but the validation rate is decreased. The signal gain for the green channel was set to 18 dB and for the blue channel it was set to 20 dB.
- Velocity center and span: The velocity center determines the mean velocity and the velocity span determines the range of velocity from the center. The center of axial velocity was 9 m/s and its span was 12 m/s. The center of radial and tangential velocity was set to 0 m/s and its span to 15 m/s. The range was selected as the smallest one, which covered all droplets.

The setting was made as a compromise between the data rate and the validation rate. After setting the data rate in middle of spray was about 10 KHz, the spherical validation rate over 95 % and velocity the validation rate was over 90 %. In Figure 5-2 is shown histogram of velocity (axial and radial) and droplets size.

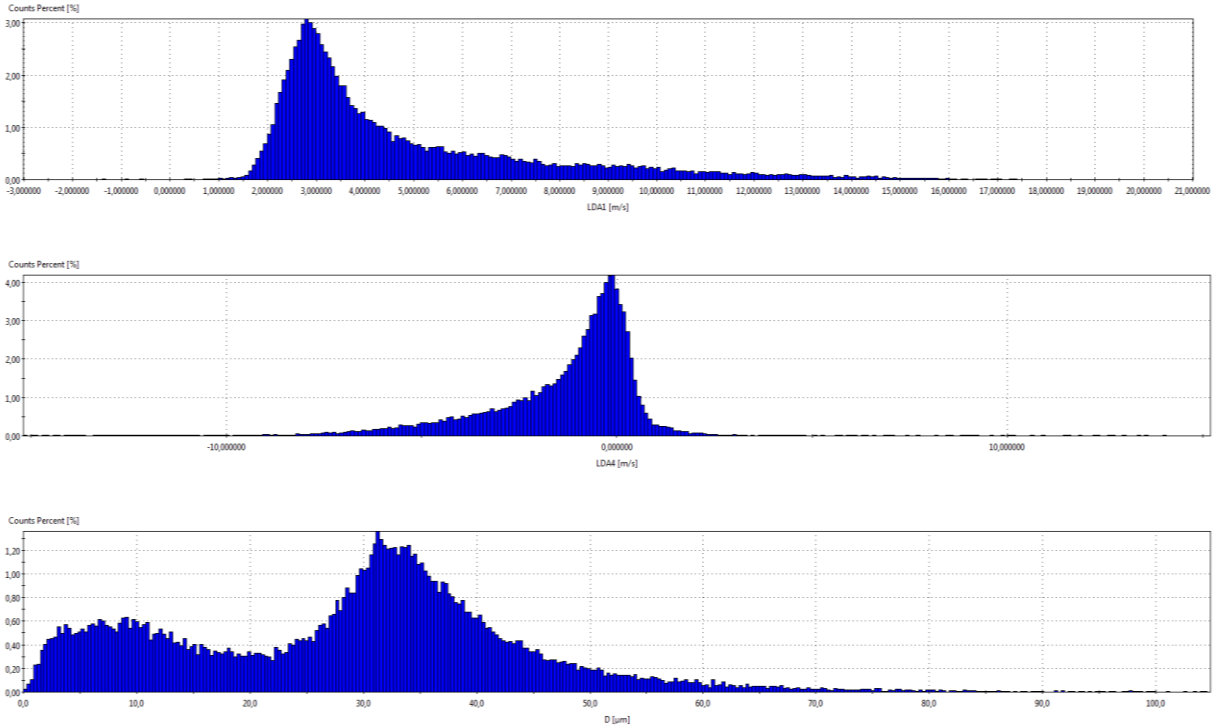

Figure 5-2 Histogram from BSA flow software, winter diesel, 50 mm downstream, 25 mm radial from spray center, inlet pressure 10 bar.

5.2. Types of atomized liquids

Several types of liquids were tested. Physical properties are summarized in Table 5-2. Fuels were selected as possible substitutes for commonly used kerosene. Low viscous diesels (arctic diesel and winter diesel), defined by EN 590 were in the investigation. Biofuels were represented by diesel with a bio component and diesel made from palm oil, both described by EN 14214. Two special liquids were used, aged winter diesel, which was basically regular winter diesel that has been stored in an open container and repeatedly atomized. Light fractions were evaporated and the density and viscosity increased. Kerosene with oil was normal kerosene with the addition of light heating oil (5 % of its volume). Properties were measured at room temperature (22 °C).

Table 5-2 The physical properties of tested liquids

Liquid	Density [kg/m^3]	Kinematic viscosity [mm^2/s]	Dynamic viscosity [mPa.s]	Surface tension [mN/m]	Mass flow rate [kg/h]
Arctic diesel	810	2.6	3.2	29	18.9
Biodiesel	831	3.9	4.6	27	20
Winter diesel	830	3.7	4.4	18	19.8
Aged winter diesel	835	5.7	6.9	49	21.7
Kerosene	785	1.5	1.9	31	17
Kerosene with oil	795	3.3	4.1	25	19.1
Palm oil	771	4	5.2	29	19.3

All measurement was made with liquids at room temperature (22 °C).

5.3. Tested atomizer

Pressure-swirl atomizer developed by PBS Velka Bites, a.s. for an ultralight aircraft engine was tested. Internal geometric dimensions corresponding to Figure 2-4 are listed in Table 5-4 Photo of the atomizer is in Figure 5-3.

Table 5-3 Operating regiments

Inlet pressure [bar]	Mass flow rate [kg/h]
5	14.1
10	18.9
15	22.3

Table 5-4 Atomizer dimensions

Geometric dimension	Value	Unit
D_0	0.36	mm
D_c	3	mm
l_c	1.41	mm
l_o	0.2	mm
A_0	0.102	mm^2
A_i	0.72	mm^2
A_c	7.07	mm^2
2θ	67	deg

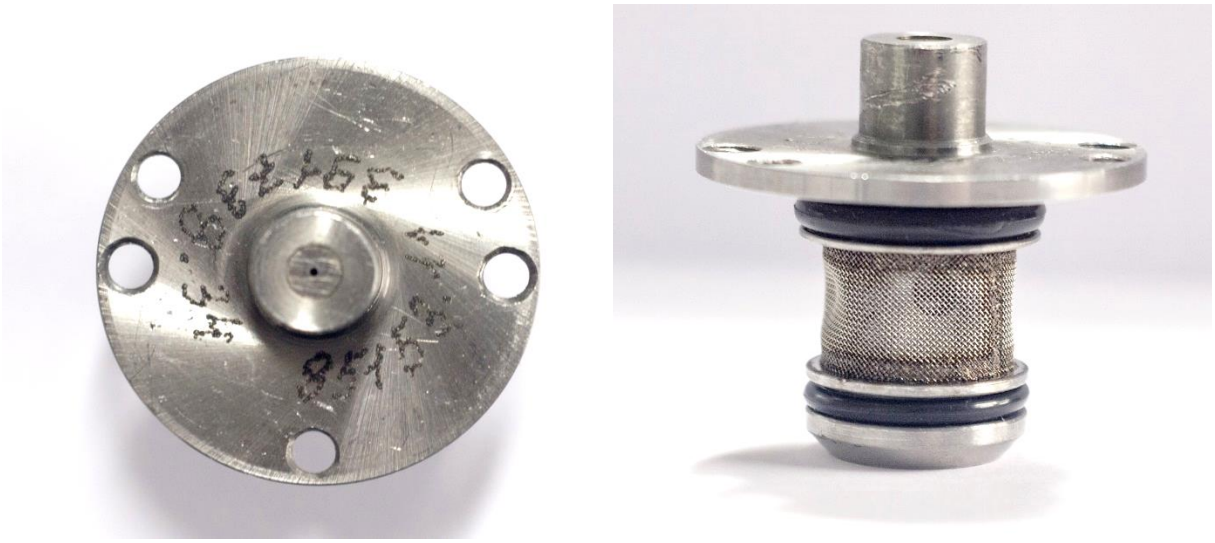

a) exit orifice b) atomizer side profile

Figure 5-3 Tested atomizer

During the tests were observed changes in mass flow rate through the atomizer depending on used liquid as shown in Table 5-2. According to [24], flow rate is depended on the liquid dynamic viscosity. Their investigation shows, that the radius of the air core is smaller for a liquid with higher viscosity, thus the flow rate through the exit orifice is higher.

Flow rate is also dependent on inlet pressure, for used pressure regiments is flow rate shown in the Table 5-3.

5.4. ISMD Calculation

Integral Sauter mean diameter (ID_{32} or ISMD) was used as single parameter to characterize global spray quality and was defined in [25] as:

$$\mathrm{ISMD} = \frac{\sum_{i=1}^{n} r_i D_{30,i}^3 f_i}{\sum_{i=1}^{n} r_i D_{20,i}^2 f_i} \tag{5.1}$$

Where r_i is radial distance, $D_{30,i}$ is volume mean diameter, $D_{20,i}$ is surface mean diameter and f_i is data rate.

6. Results

This chapter describes the results from the measurement of the pressure-swirl atomizer.

6.1. Visualization of spray

For the first estimate of spray behavior, photographs of spray were made. Pair of photographs was made for every pressure value, with a side flash and with background flash. The camera canon 300D and the objective Canon EF 100 mm f/2.8 USM Macro were used for all photographs. For the side flash was expose time 1/160 s and f-stop f/8. The background flash was diffused by a sheet of paper, the camera was set to expose time 1/100 s and f-stop f/4.5.

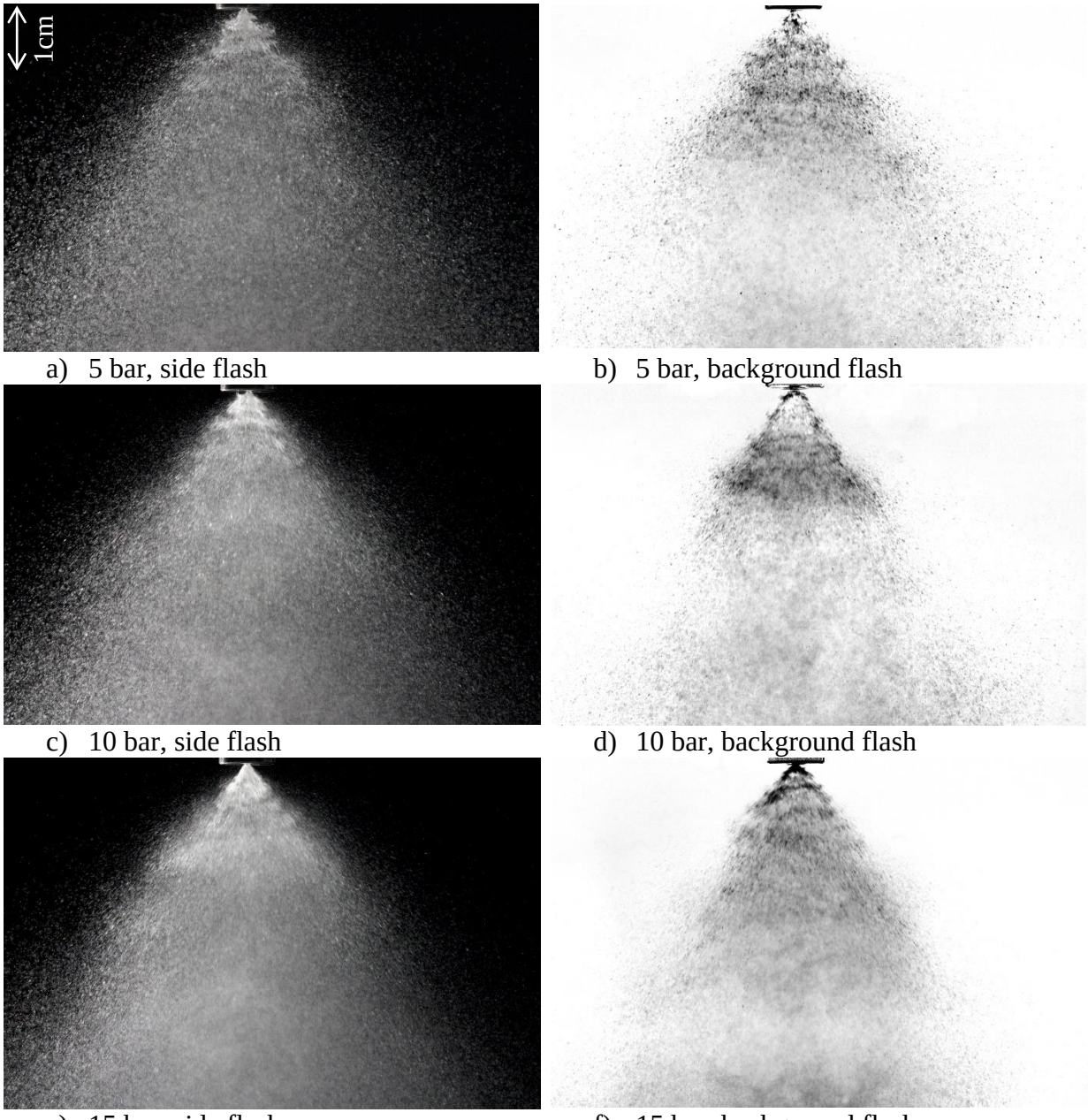

a) 5 bar, side flash
b) 5 bar, background flash
c) 10 bar, side flash
d) 10 bar, background flash
e) 15 bar, side flash
f) 15 bar, background flash

Figure 6-1 Spray visualization

From a visual point of view is the spray is axially symmetric. The liquid sheet disintegrates into ligaments and drops in a very short distance from the atomizer orifice. Liquid break up is complete about 20 mm downstream from the final orifice for all investigated pressures. The cone angle appears to be independent of the pressure.

6.2. Spray symmetry

Spray was measured 50 mm downstream at an inlet pressure of 10 bar with kerosene in four axis, the evaluation was made using their half-axes. In Figure 6-2 the SMD profile is shown, which is fairly axisymmetric in all radial distances and axial velocity profile, which illustrates some cases of slight asymmetry. This difference is due to imperfect atomizer geometrics or different optical access from the measuring point to receiving optics. For further investigation, symmetrical spray will be assumed.

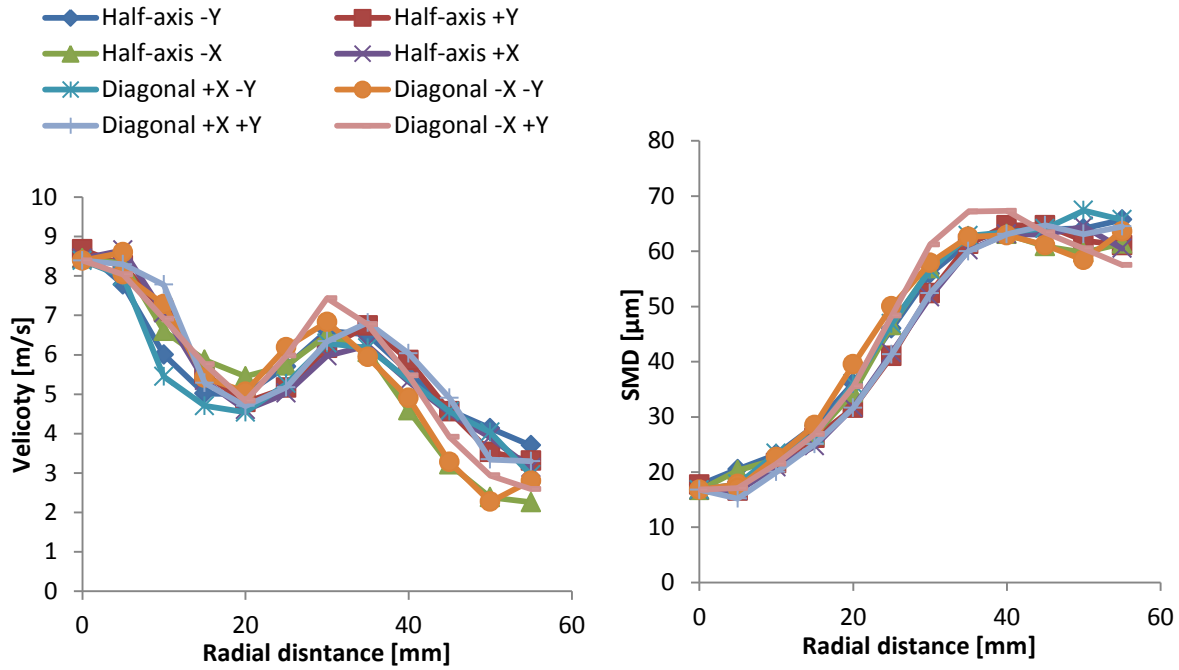

a) Axial velocity b) SMD

Figure 6-2 Spray symmetry

6.3. Spray structure

Acquired data were sorted by droplets diameter into 4 classes and plotted into Figure 6-3. The smallest particles are in the class 0-10 µm, while the largest are in the class 50-105 µm. The measurement was made at a pressure of 15 bar and 50 mm downstream from the nozzle orifice with winter diesel.

The largest particles with the largest momentum are less decelerated by surrounding air and their both axial and radial velocities are much higher across the whole profile. Compared to the other classes, the velocity peak of the largest particles is moved from the center of spray into the edge of the spray, where the liquid sheet was disintegrated. Around this position there is also the largest number of these particles. In the center of the spray, larger particles (above 20 µm) are almost absent, their number is growing with radial distance from the center to the disintegrated liquid sheet, whereas the number of smaller particles is decreases.

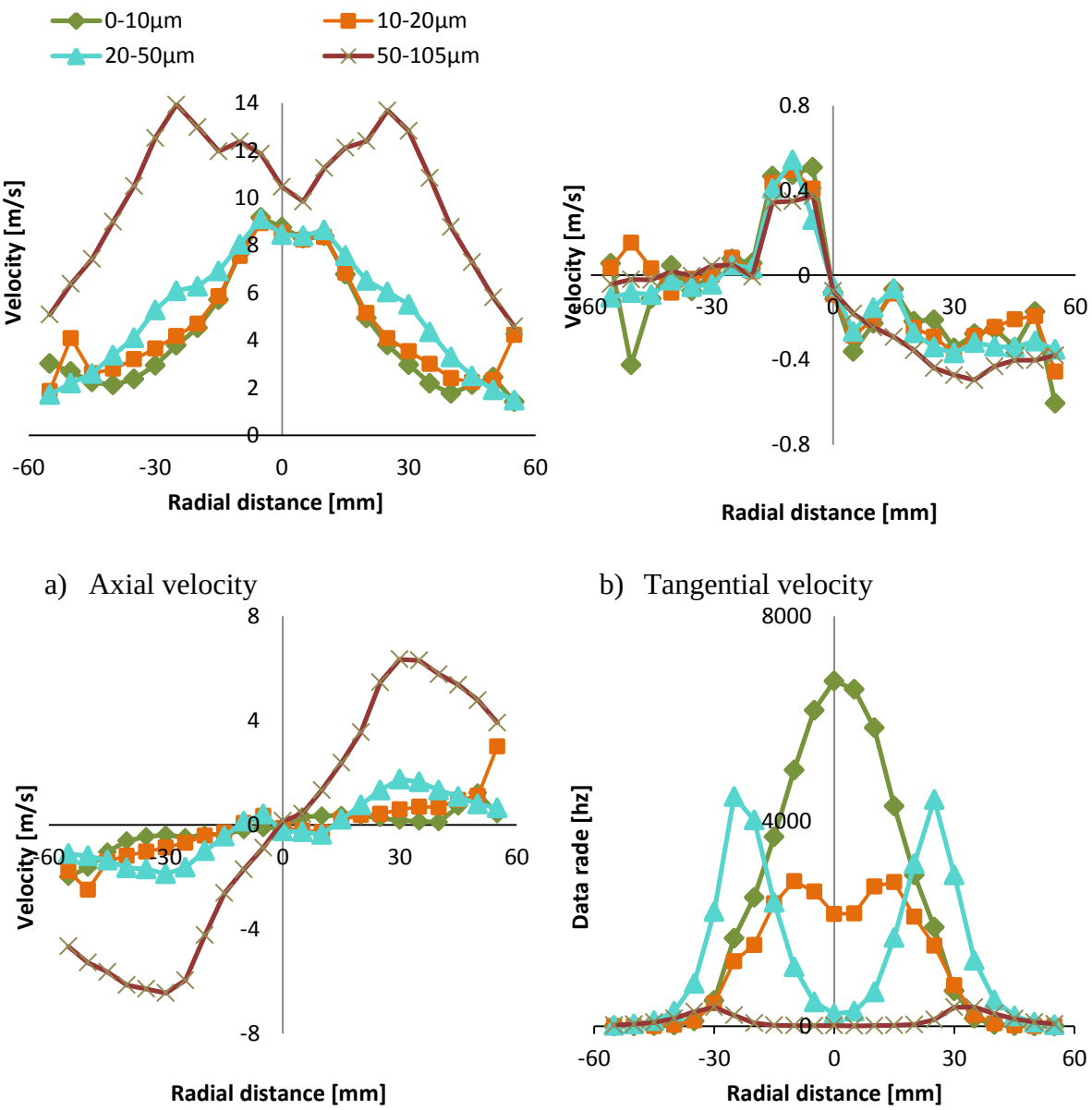

a) Axial velocity

b) Tangential velocity

e) Radial velocity

d) Count of particles per second

Figure 6-3 Sorted particles into classes

6.4. Cone angle

Cone angle was derived from cumulative volume distribution across the profile in radial direction. Measurement was made 50 mm downstream from exit orifice with winter diesel. The criterion which determines the cone angle was set to border of 90 % of all liquid volume inside the spray as shown in Figure 6-4. The final spray cone angle was 67° and with increasing pressure remains practically unchanged, but volume distribution inside spray is changes. With increasing pressure the liquid volume moves from the center to the spray edge. It follows that with increasing inlet pressure there is more liquid volume concentrated in the

liquid sheet. Due to small liquid volume near the center spray may be regarded as a hollow-cone.

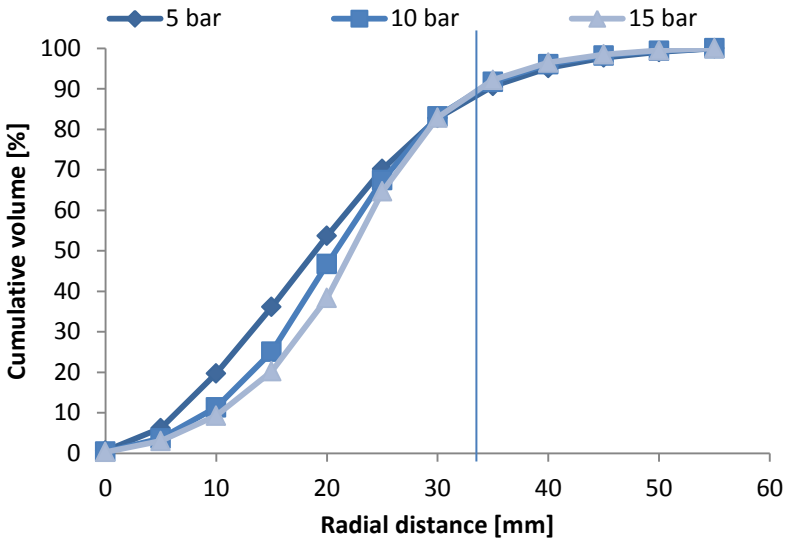

Figure 6-4 Liquid volume distribution

According to equation 2.5, the cone angle should be dependent to inlet pressure. Increases in pressure should result in a wider cone angle. This behavior was not observed in this thesis but assuming that the change of liquid distribution corresponds to the change of an effective cone angle (a greater amount of volume is exposed to a larger area) thus the cone angle increases with inlet pressure.

6.5. Axial distance

Measurements were made at inlet pressure 10 bar with winter diesel. Results were evaluated in normal and relative axial distances. Relative radial distance was calculated as:

$$r^*_i = \frac{r_i}{z_i} \tag{6.1}$$

where r^*_i is relative radial distance, r_i is radial distance and z_i is axial distance.

Figure 6-5 shows a dependency SMD and velocities on axial distance. With increasing axial distance, both axial and radial velocity decreases. Between 25 mm and 50 mm the velocity difference is greatest, due to the rapid deceleration of small particles with a small momentum. Particles in the center of the spray keep their velocities through all measured axial distances. Tangential velocity was only slightly influenced.

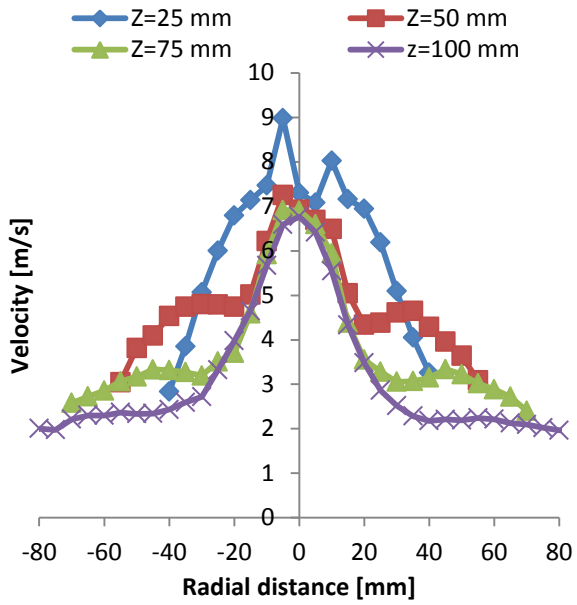

a) Axial velocity

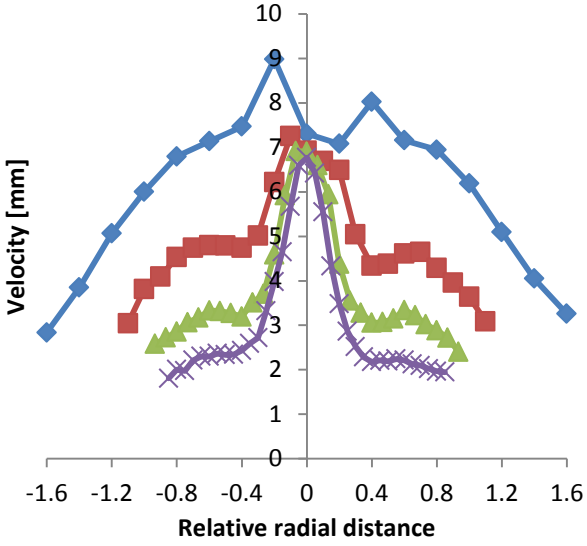

b) Relative axial velocity

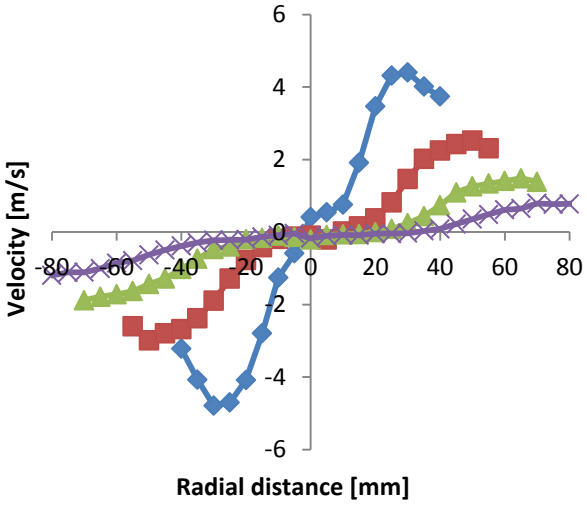

c) Radial velocity

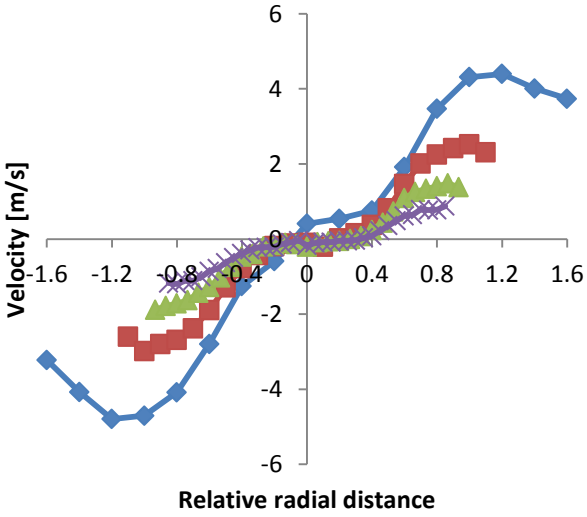

d) Relative radial velocity

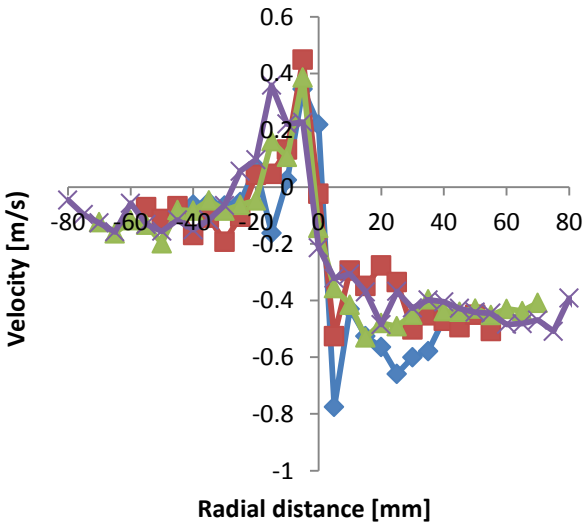

e) Tangencial velocity

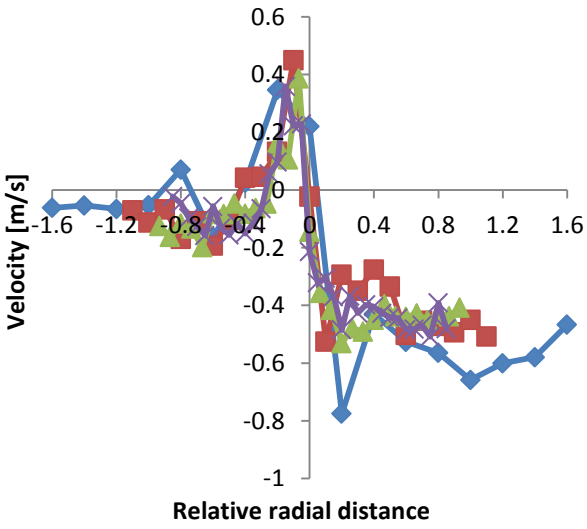

f) Relative tangencial velocity

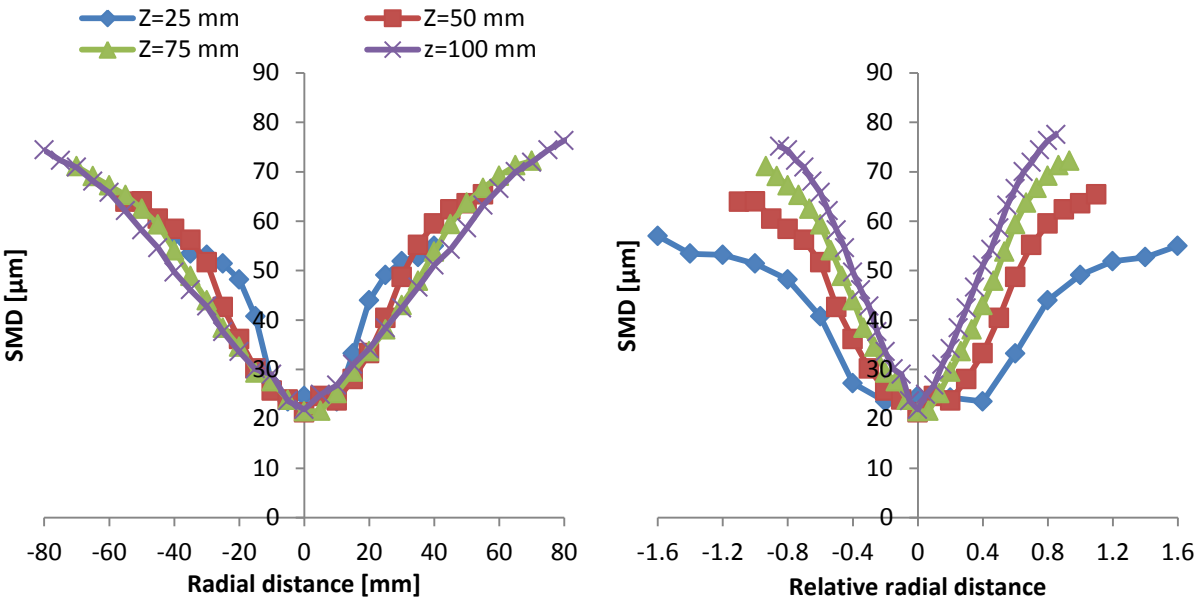

g) SMD h) Relative SMD

Figure 6-5 Influence of axial distance

SMD with increasing axial distance is growing as shown in Figure 6-5. ISMD was calculated resulting in Table 6-1. SMD is increases almost linearly through all the axial distance. This behavior was observed in literature [26, 27], where the major role was assigned to droplets coalescence and the effect of acceleration or deceleration. The Figure 6-5 h) shows dependency SMD on relative radial distance. In the center of the spray there is a low droplets density (hollow-cone spray is assumed) thus less droplets will collide and the smallest drops are moved from border to the spray center thus SMD is lowering. With increasing radial distance, spray density is growing and more drops will collide thus SMD will be increased.

Table 6-1 Influence of axial distance on ISMD

Axial distance [mm]	ISMD [µm]
25	42.4
50	45.6
75	49.0
100	52.9

6.6. Inlet pressure influence

Measurements were made with arctic diesel 50 mm downstream of the exit orifice.

Which increasing liquid pressure SMD is rapidly decreasing and axial velocity is increasing (shown in Figure 6-6), as was mentioned in chapter 2.4. Where disintegrated liquid sheet is expected, radial velocity is increasing with increasing liquid pressure. In Table 6-2 Pressure influence is shown dependency of ISMD on initial pressure and it fully corresponds to Figure 6-6.

Table 6-2 Pressure influence on ISMD

Pressure [bar]	ISMD [µm]
5	54.1
10	46.2
15	41.6

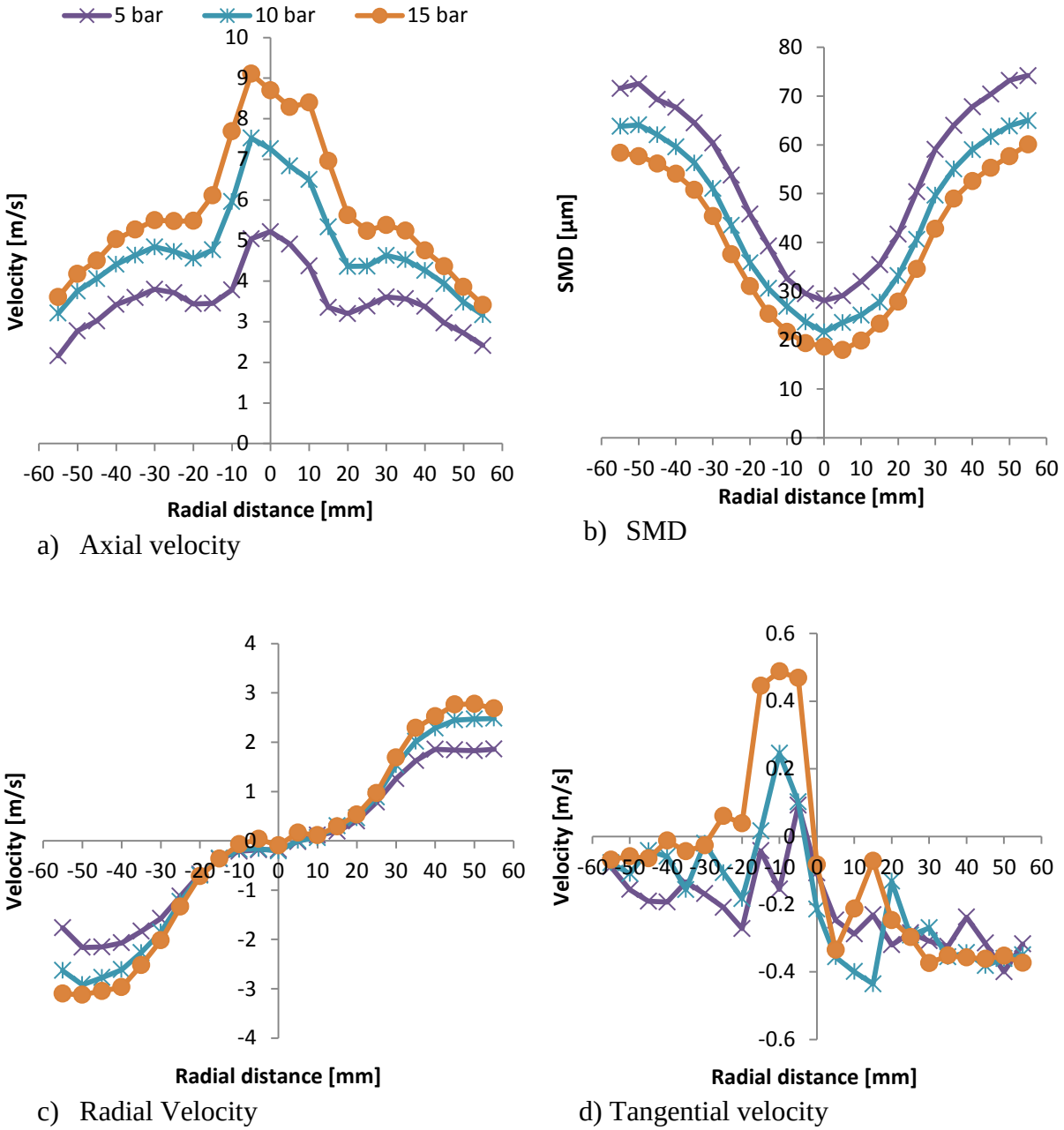

a) Axial velocity

b) SMD

c) Radial Velocity

d) Tangential velocity

Figure 6-6 Pressure influence

6.7. Influence of liquid properties

Several kinds of liquids (Table 5-2) were tested to describe the influence of liquid properties in changes of SMD and axial velocities. All tests were made 50 mm downstream of the exit orifice. The liquid inlet pressure was set to 10 bar. Figure 6-7 shows dependency of SMD and axial distance on radial distance for every tested liquid.

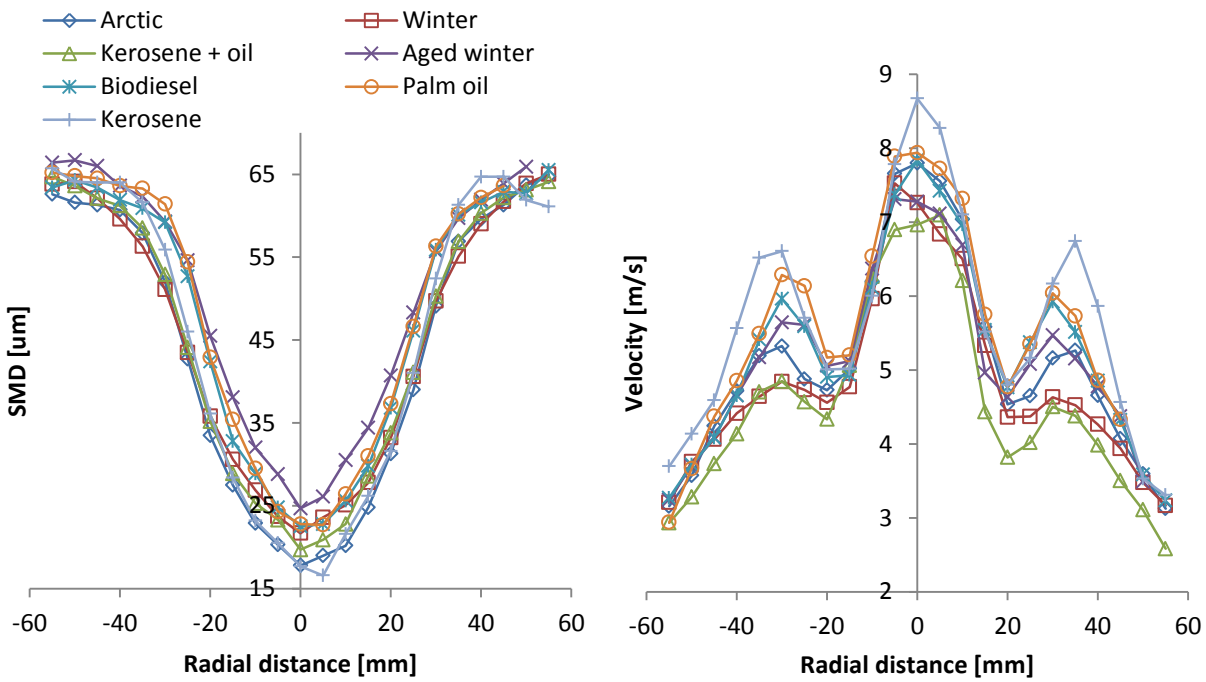

a) SMD b) Axial velocity

Figure 6-7 Influence of liquid properties

Due to a small disparity in liquids density, it is assumed that only viscosity and surface tension are responsible for changes in SMD and axial velocity. Kerosene with the lowest viscosity has the highest axial velocity in both spray center and spray cone. On the other hand, kerosene with addition of oil has the smallest axial velocity.

Table 6-3 shows a dependence of ISMD on different liquids. Kerosene and Arctic diesel, both with low viscosity, have significantly smaller ISMD, while more viscous aged winter diesel had considerably larger ISMD. Both biofuels, the biodiesel and the palm oil, have higher viscosity hence ISMD than common fuels like a kerosene or winter diesel. This result was anticipated from list of correlations in Table 2-2. However, some liquids exhibit disparities between the measured data and theory. Arctic diesel with slightly higher both viscosity and surface tension has lower ISMD than kerosene. Biodiesel and winter diesel have almost same viscosity, but lower surface tension of winter diesel means smaller ISMD exactly as the theory goes.

Table 6-3 Influence of liquid properties on ISMD

Liquid	ISMD [μm]
Arctic diesel	44.2
Kerosene	46.3
Winter diesel	46.9
Kerosene + oil	50.7
Biodiesel	50.7
Palm oil	52.6
Aged winter diesel	53.1

With regard to replacement of kerosene by alternative fuels, SMD have most dominant effect in terms of atomization (heating value and other important aspect of combustion are not discussed in this thesis). From results in Table 6-3 we can conclude, that is possible to substitute kerosene with low viscous diesels such as Arctic diesel and in some cases with winter diesel. All biofuels have higher viscosity thus larger ISMD and their application is not possible without modification of atomizer parameters or operating conditions.

7. Conclusion

7.1. Atomizer performance

In the present work, the performance of the pressure-swirl atomizer in different pressure regiments with various liquid was investigated.

- The spray cone angle was found to be independent of injection pressure. But internal volume distribution is dependent on pressure.
- Sauter mean diameter increases with increasing downstream distance. This phenomenon was attributed to droplets collisions.
- With increasing inlet pressure SMD is rapidly decreases.
- Liquid viscosity was found to have the largest influence on SMD, with increasing viscosity SMD is increases.
- Surface tension has negative effect on SMD
- Biofuels had significantly higher SMD due to a higher viscosity and surface tension.

The issue of replacement kerosene with biofuels was examined in terms of atomization quality (SMD) and all biofuels had higher SMD than kerosene, expect low viscous diesels without bio addition. If the biofuels will be used without modification of operating conditions, less performance and more pollution will be produced. A solution is to reduce the biofuels viscosity by increasing its temperature or changing operating conditions such as increases in injection pressure.

7.2. Goals

The main goals of this thesis were fulfilled in chapters:

- Study of relevant publications to pressure-swirl atomizers (chapter 2)
- Modification of test equipment for operation of pressure-swirl atomizers and verify the accuracy of the sensors (chapter 4)
- Preparation and setup of optical measuring system (chapter 5)
- Measurement of selected characteristics of pressure-swirl atomizer (chapter 6)
- Analysis of results, description sprays and evaluating the operating conditions. Graphical presentation of results (chapter 6)

Accomplishment of all goals took over a year of work, while the most of time was spent to learning to operate and satisfactory setup of PDA measuring system. The theoretical part of this work is not discussed in detail because this topic has previously been elaborated in masters thesis and the focus of this thesis was in the experimental chapters. One pressure-swirl atomizer was tested, the initial plan was to test and compare several pressure-swirl atomizers, but due to the late delivery of additional atomizers it was not possible to done it on time. These atomizers will be measured and compared within next work.

List of symbols

Roman symbols

A	Liquid surface	$[m^2]$
A_c	Area of swirl chamber	$[m^2]$
A_i	Total area of inlet holes	$[m^2]$
A_o	Area of orifice	$[m^2]$
Cd	Discharge coefficient	[-]
D	Drop diameter	[m]
$D_{0.1}$	Drop diameter that 10% of total liquid volume is in drops of smaller diameter	[m]
$D_{0.5}$	Drop diameter that 50% of total liquid volume is in drops of smaller diameter	[m]
$D_{0.632}$	Drop diameter that 63.2% of total liquid volume is in drops of smaller diameter	[m]
$D_{0.9}$	Drop diameter that 90% of total liquid volume is in drops of smaller diameter	[m]
D_{10}	Arithmetic mean diameter	[m]
D_{20}	Area mean diameter	[m]
D_{21}	Area-length mean diameter	[m]
D_{30}	Volume mean diameter	[m]
D_{31}	Mean evaporative diameter	[m]
D_{32}	Sauter mean diameter	[m]
D_{43}	De Broukere diameter	[m]
D_c	Swirl chamber diameter	[m]
D_0	Diameter of orifice	[m]
E	Measurement error	[%]
E_a	Surface energy	[J]
f_i	Data rate	[Hz]

FN	Flow number	[-]
h_0	Liquid sheet thickness at the nozzle tip	[m]
k	Sheet number	[-]
l_c	Length of swirl chamber	[m]
l_0	Length of orifice	[m]
$\dot{m}_l$	Liquid mass flow rate	[kg/s]
t = FT	Film thickness in final orifice	[m]
Δt	Signal shift	[s]
Δp_l	Injector pressure differential	[Pa]
Q	Fraction of total volume	[-]
r_i	Radial distance	[m]
U_e	Average tangential velocity of the fluid through the orifice	[m/s]
U_0	Velocity of the liquid at the atomizer tip	[m/s]
V_e	Average axial velocity of the fluid through the orifice	[m/s]
v_{eff}	Effective sheet velocity	[m/s]
v_{pot}	Potential sheet velocity	[m/s]
We	Weber number	[-]
z_i	Downstream distance	[m]

Greek symbols

θ	Spray cone half angle	[deg]
ϑ	Kinematic viscosity	[m^2/s]
μ	Dynamic viscosity	[mPa·s]
ρ_l	Liquid density	[kg/m^3]
ρ_a	Air density	[kg/m^3]
σ	Surface tension	[kg/s^2]
θ	Spray cone half angle	[deg]

ϕ	Velocity coefficient	[-]

Abbreviations

LDA	Laser Doppler anemometry	
PDA	Phase Doppler anemometry	
SMD	Sauter mean diameter	[m]
ISMD	Integral Sauter mean diameter	[m]

Bibliography

[1] Lefebvre, A. H., and Ballal, D. R., 2010, "Gas turbine combustion alternative fuels and emissions," Taylor & Francis,, Boca Raton, pp. 1 online resource (xix, 537 p.).

[2] Lefebvre, A., 2000, "Fifty years of gas turbine fuel injection," Atomization and Sprays, 10(3-5), pp. 251-276.

[3] Khavkin, Y., 2004, The Theory and Practice of Swirl Atomizers, Taylor & Francis.

[4] Lefebvre, A., 1995, "The role of fuel preparation in low-emission combustion," Journal of engineering for gas turbines and power, 117(4), pp. 617-654.

[5] "Dantec Dynamics. [online]," http://www.dantecdynamics.com.

[6] Ashgriz, N., and SpringerLink (Online service), 2011, "Handbook of atomization and spraystheory and applications," Springer,, New York, pp. xvi, 935 p.

[7] 2012,"Hollow conen nozzles,"Lechler,.http://www.lechler.de/isbin/intershop.static/WFS/LechlerDEShopSite/LechlerDEShop/en_US/PDF/05_service_support/industrie/katalog/englisch/2_hohlkegel_Lechler_GB.pdf.

[8] Rizk, N. K., and Lefebvre, A. H., 1985, "Internal flow characteristics of simplex swirl atomizers," Journal of Propulsion and Power, 1(3), pp. 193-199.

[9] Rizk, N., and Lefebvre, A., 1987, "Prediction of velocity coefficient and spray cone angle for simplex swirl atomizers," International Journal of Turbo and Jet Engines, 4(1-2), pp. 65-74.

[10] Ohnesorge, W. v., 1936, "Formation of drops by nozzles and the breakup of liquid jets," Z. Angew. Math. Mech, 16(4), pp. 355-358.

[11] Radcliffe, A., 1960, Fuel Injection, High Speed Aerodynamics and Jet Propulsion, Princenton University Press, Princenton, N.Y.

[12] Jasuja, A. K., 1979, "Atomization of crude and residual fuel oils," Journal of Engineering for Power-Transactions of the Asme, 101(2), pp. 250-258.

[13] Lefebvre, A., 1987, "The prediction of Sauter mean diameter for simplex pressure-swirl atomisers," Atomisation Spray Technology, 3, pp. 37-51.

[14] Simmons, H. C., and Harding, C. F., 1981, "Some effects of using water as a test fluid in fuel nozzle spray analysis," Journal of Engineering for Power-Transactions of the Asme, 103(1), pp. 118-123.

[15] Babu, R. K., Narasimhan, M. V., and Karayanaswamy, K., 1982, "Prediction of Mean Drop Size of Fuel Sprays from Swirl Spray Atomizers," Proceedings of the second International Conference on Liquid Atomisation and Spray SystemsMadison, Wisconsin, pp. 99-106.

[16] Kennedy, J., 1986, "High Weber number SMD correlations for pressure atomizers," Journal of engineering for gas turbines and power, 108(1), pp. 191-195.

[17] Wang, X. F., and Lefebvre, A. H., 1987, " Mean drop sizes from pressure-swirl nozzles," Journal of Propulsion and Power, 3(1), pp. 11-18.

[18] Couto, H., Carvalho, J., and Bastos-Netto, D., 1997, "Theoretical formulation for Sauter mean diameter of pressure-swirl atomizers," Journal of Propulsion and Power, 13(5), pp. 691-696.

[19] Musemic, E., and Walzel, P., "Swirl Atomizers with Coanda Deflection Outlets."

[20] Zhang, Z., 2010, LDA Application Methods: Laser Doppler Anemometry for Fluid Dynamics, Springer.

[21] Albrecht, H.-E., 2003, Laser doppler and phase doppler measurement techniques, Springer, Berlin ; New York.

[22] Lading, L., Wigley, G., and Buchhave, P., 1994, Optical diagnostics for flow processes, Plenum Press.

[23] Yeh, Y., and Cummins, H. Z., 1964, " Localized fluid flow measurements with an He–Ne laser spectrometer," Applied Physics Letters, 4(10), pp. 176-178.

[24] Wimmer, E., and Brenn, G., 2013, "Viscous flow through the swirl chamber of a pressure-swirl atomizer," International Journal of Multiphase Flow.

[25] Jedelsky, J., Jicha, M., Slama, J., and Otahal, J., 2009, "Development of an Effervescent Atomizer for Industrial Burners," Energy & Fuels, 23, pp. 6121-6130.

[26] Zhao, Y., Li, W., and Chin, J., 1986, "Experimental and analytical investigation on the variation of spray characteristics along radial distance downstream of a pressure swirl atomizer," Journal of engineering for gas turbines and power, 108(3), pp. 473-478.

[27] Reddy, K. U., and Mishra, D. P., 2008, "Studies on spray behavior of a pressure swirl atomizer in transition regime," Journal of Propulsion and Power, 24(1), pp. 74-80.